NASA-CR-120782
AI-71-40

FINAL REPORT

LITHIUM HYDRIDE SHIELD SEGMENT FABRICATION

By
F. H. Welch

ATOMICS INTERNATIONAL DIVISION
NORTH AMERICAN ROCKWELL CORPORATION

Prepared for
NATIONAL AERONAUTICS AND SPACE ADMINISTRATION
NASA LEWIS RESEARCH CENTER
CONTRACT NAS 3-13466
L. Kaszubinski, Project Manager

Requests for copies of this report should be referred to:

National Aeronautics and Space Administration
Scientific and Technical Information Facility
P. O. Box 33
College Park, Md. 20740

NASA-CR-120782
AI-71-40

FINAL REPORT

LITHIUM HYDRIDE SHIELD SEGMENT FABRICATION

By
F. H. Welch

ATOMICS INTERNATIONAL DIVISION
NORTH AMERICAN ROCKWELL CORPORATION
8900 DeSoto Avenue
Canoga Park, California 91304

Prepared for
NATIONAL AERONAUTICS AND SPACE ADMINISTRATION
SEPTEMBER 3, 1971

CONTRACT NAS 3-13466
NASA LEWIS RESEARCH CENTER
CLEVELAND, OHIO

L. Kaszubinski, Project Manager

FOREWORD

The work described here was performed by the Atomics International (AI) Division of the North American Rockwell Corporation (NR), under NASA Contract NAS 3-13466, with Mr. L. Kaszubinski, NASA Lewis Research Center, as Project Manager.

CONTENTS

APPENDICES

TABLES

FIGURES

FIGURES

ABSTRACT

Four shield segments were designed, built, and filled with lithium hydride (LiH) by a casting process. The segments were sectors of a right circular cylindrical annulus, which will be used for tests in the NASA Lewis Research Center Zero Power Reactor. The cylindrical annulus, 29.4 in. (0.747 m) in diameter and 36.4 in. (0.925 m) high, contained ~352 lb (160 kg) of high-purity (>98%) natural lithium hydride in the 5.22-in. (0.133-m) thick walls. Three of the four segments contained penetrations through the lithium hydride, which will be used in tests of radiation streaming through ducts.

I. SUMMARY

Four shield segments were designed, fabricated, and filled with natural LiH, by casting into welded stainless steel containers. These segments were sectors of a right circular cylindrical annulus, 36.4 in. (0.925 m) high, with an outer diameter of 29.4 in. (0.74 m) and an inner diameter of 18.96 in. (0.482 m). Each sector was a different shape, and three of the four segments contained penetration tubes in the central region. These penetration tubes were straight or curved pipes, of 1.0, 2.0, or 3.5 in. (25.4, 50.8, or 88.9 mm) diameter.

A special casting support structure was built to hold the containers, and to minimize distortion during the casting cycle. Other casting hardware needed for the process also was built.

A trial segment was cast to establish the extent and nature of the distortions which might occur during a casting cycle, and to determine changes that might be needed to improve the final castings. Examination of the trial segment revealed that the most serious distortion was a "twist," over the length of the segment. Also, a small casting void was found at the top of the segment, under the LiH filler tube.

The addition of shims to the casting support fixture, and the use of a precise technique for installing the segments in the fixture, corrected the twist in the final three segments. In the side walls, the maximum "pull-in" after casting was 0.116 in. (2.94 mm), and the maximum bulge was 0.046 in. (1.17 mm). Evaluation of the dimensions of the three production castings showed that they could be used with the trial casting in the final assembly without interference.

It was postulated that the casting void was caused by excessive heat loss from the top plate, allowing a premature freezing of the LiH at the plate while the LiH in the segment was still molten. An additional thermocouple was placed in the LiH, at the level of the top plate, to detect the premature freezing; and a copper heat diffuser disc was placed on the top plate, around the filler tube to provide a more uniform heat distribution. With this technique, the voids were eliminated in the final two castings.

Radiography of the cast LiH revealed cracks in the crystalline material. The stainless steel honeycomb which was placed in the containers successfully prevented the propagation of the cracks to unacceptable size.

Void volume measurements indicated that the segments contained LiH of 93.6 to 94.2% of theoretical density, which was greater than the 93% minimum goal.

Chemical analyses showed the LiH to be >98% pure; and isotopic analyses established that the lithium contained 7.49 at. % of the Li^6 isotope, which is the naturally occurring amount.

II. INTRODUCTION

The objective of this program was to fabricate a cast lithium hydride shield, consisting of four segments of an annular shield conforming to the dimensional and quality requirements of the NASA drawings and specifications (Appendices 1 and 2).

The zone-cooling technique, of progressively freezing the LiH from the bottom upwards to accommodate the 20% shrinkage of the freezing lithium hydride, was selected to produce these castings. Lithium hydride shields, weighing up to 1700 lb (770 kg), had been fabricated with this casting technique, in connection with the Atomic Energy Commission's SNAP Reactor Program (Reference 1 and 2). However, the segmented annulus required for this program was an unusual shape, which had not been cast previously. Because of the possibility of severe stress patterns occurring during the casting process that could produce large distortions, provisions were made to fabricate a trial casting of one of the shield segments. The results of the evaluation of the trial casting would provide the basis for revising the casting process, the fixturing, and the NASA shield specification for the production of the annular shield.

The program was conducted in two phases. Phase I consisted of:

1) Design and fabrication of all shield segment containers
2) Design and fabrication of the shield segment holding fixture and casting hardware
3) Trial casting of one of the shield segments
4) Nondestructive testing of the trial casting, that included:
    a) Void volume measurements
    b) X-ray radiographic examination
    c) Helium leak tests
    d) Comprehensive dimensional measurements
    e) Chemical and isotopic analysis of the lithium hydride.

Phase II consisted of the fabrication and nondestructive testing of only three of the four required shield segments, because the trial casting was accepted by NASA as the fourth segment.

III. DESIGN AND FABRICATION OF COMPONENTS

A. DESIGN OF SHIELD SEGMENTS

The design of the four shield segments was based on the NASA-supplied drawings and a LiH shield specification. The four segments were sections of a right circular annular cylinder, 36.4 in. (0.925 m) high, with an outer diameter of 29.4 in. (0.747 m) and an inner diameter of 18.96 in. (0.482 m).

The shape and relationship of the shield segments are shown in Figure 1. The segments were shaped so their butting surfaces form tangent lines with the NASA reactor source. Three of the four segments contained penetrations. Segment No. 7, the largest in size, contained the 3.5 in. (88.9 mm) diameter penetration. Segments No. 1 and 2, containing the 2.0 in. (50.8 mm) and the 1.0 in. (25.4 mm) diameter penetrations, respectively, were identical in size and shape. Segment No. 3 was the smallest in size, and contained no penetration.

Each segment contained a stainless steel, square-cell, honeycomb matrix, fabricated from 0.001-in. (0.0254-mm) thick foil. The honeycomb was oriented with the length of the cell parallel to the axis of the shield annulus. The cell size was 1 in. (25.4 mm), and the walls of the cell were perforated with 0.5 in. (12.7 mm) holes on 0.75 in. (19.0 mm) centers. The function of the honeycomb matrix was to prevent the propagation of cracks in the crystalline LiH, and to orient the cracks in such a manner as to place them at angles to the neutron source.

The shield segment containers were constructed of Type 304 stainless steel, with gas tungsten arc welded seams. The curved inner and outer walls and the flat side walls were 0.078 in. (1.98 mm) thick. The top and bottom plates were 0.375 in. (9.5 mm) and 0.75 in. (19.1 mm) thick, respectively.

No changes were required in the geometry or dimensions of the segments, to adapt them to the LiH casting process, although stainless steel sheathed, MgO insulated, Chromel-Alumel thermocouples, required for temperature monitoring of the LiH during the heating and cooling cycle of the casting process, were added to the interior of the segments.

The drawings for the fabrication of the segments and fittings, and the construction, inspection, and quality control requirements, are listed in the Appendix 1.

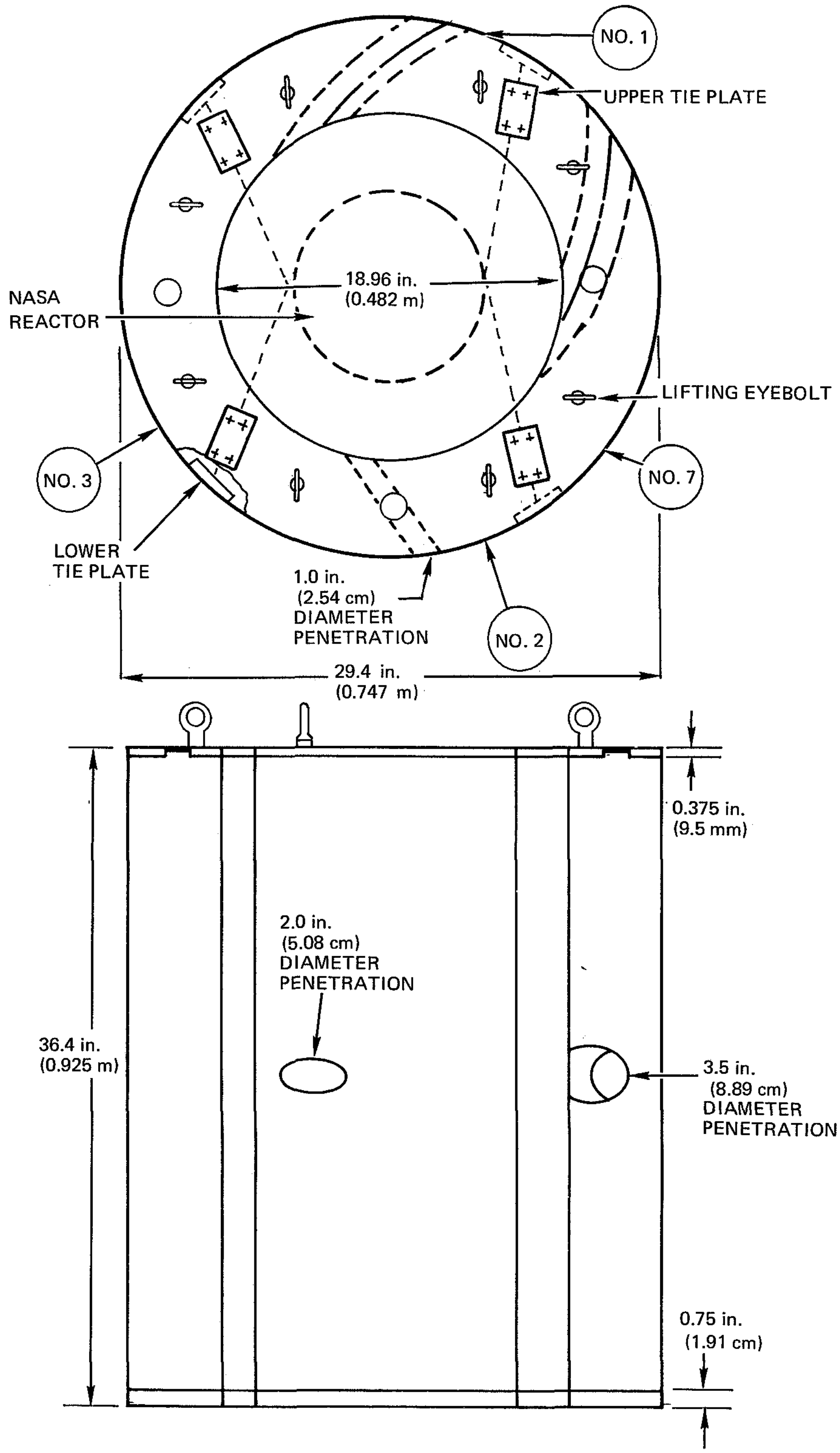

Figure 1. Shield Geometry

B. DESIGN OF THE CASTING HARDWARE AND ACCESSORIES

In addition to the casting hardware described in Appendix 3, it was necessary to provide a restraining fixture to minimize the distortion of the segments during the heating and cooling cycle. Based upon the examination of previous shield castings (Reference 1 and 2), the walls of the container had a tendency to distort inward during the casting cycle. Several reasons for this action have been postulated: (1) the contracting LiH, adhering to the container walls, pulls the walls inward, or (2) the contracting LiH creates a void which produces a pressure differential between the inside and the outside, causing the wall to distort inward.

Because inward movements would not affect the assembly of the segments into the required annulus, no attempt was made to prevent these movements. The casting support structure was designed to prevent the inner concave surface and the side plates of the segment from bulging outward, and to maintain alignment of the top and bottom plates. Because of the various geometries of the segments to be accommodated in the structure, adaptor blocks were provided which could be shimmed to support the flat sides of the segments. Each segment was held tightly in the cavity formed by the casting support cylinder and the adaptor blocks by heavy straps at the top and bottom of the segment. Figure 2 is an illustration of the casting support structure, which is a heavy-wall cylindrical spool with a cavity for mounting the segment between the two adaptor blocks.

The remaining casting hardware, the safety container, framework, reservoir, and filler tube - bellows assembly are illustrated in Figure 3. These items were designed, using previously established techniques (Reference 1).

Trim heaters were used to provide the fine control of the temperatures in the filler tube - bellows assembly, the reservoir, and the central cavity of the casting support structure. These heaters were coiled, stainless steel sheathed, MgO insulated, Nichrome wire. The filler tube and reservoir heaters were used to keep the LiH molten in these regions until all freezing was completed in the shield segment. The trim heater located at the top of the central cavity of the casting support structure was used to maintain the temperature on the inner surface of the cavity equal to the temperature on the outer surface of the segment, which is heated by the casting furnace. Equal temperatures on the two surfaces promote a symmetrical LiH freezing pattern.

Appendix 1 contains a list of the drawings for the casting hardware.

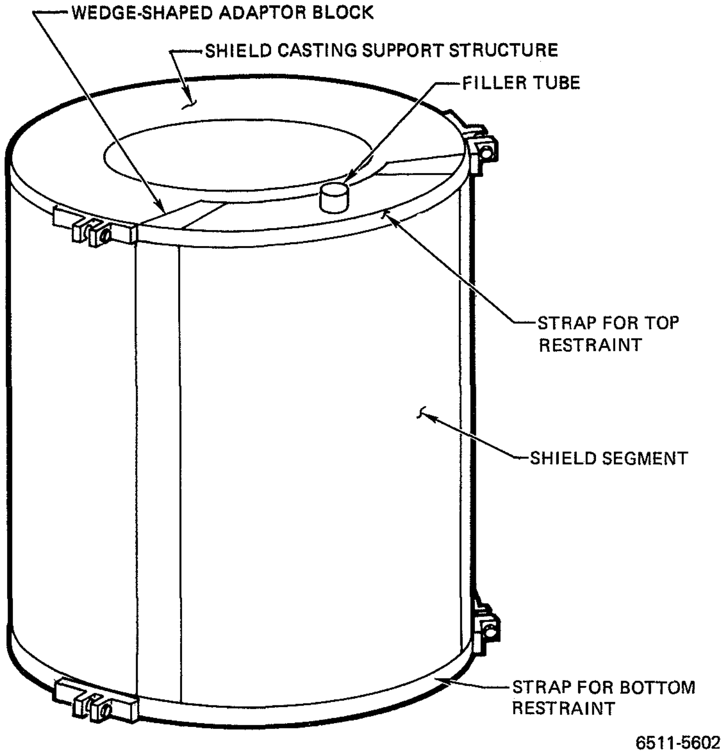

Figure 2.
Casting Support Fixture and Segment

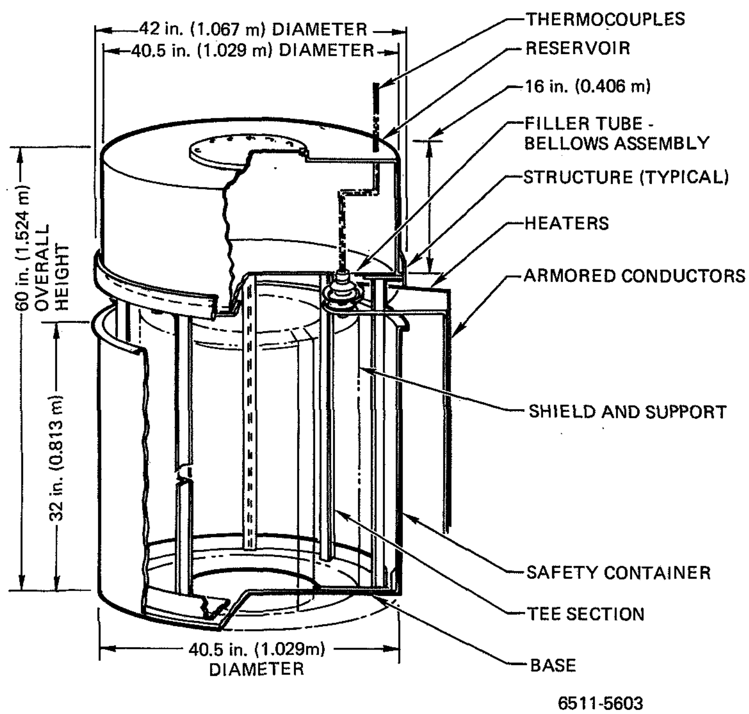

Figure 3.
LiH Shield Casting Hardware

C. SHIELD SEGMENT ASSEMBLY

The shield containers were procured as assembled cans, except for the top plate and the penetration tube. The honeycomb matrix was installed with the cells of the honeycomb oriented parallel to the height of the segment. The rectangular prism of honeycomb was hand trimmed with scissors into a trapezoidal prism, slightly larger than the internal dimensions of the container. The honeycomb was hand formed to the shape of the inside of the container, and was slid into place (Figure 4). As viewed from the top, the honeycomb cells formed a diamond-shaped pattern, slightly compressed at the inner side and slightly expanded at the outer side (Figure 5).

Using the penetration tube hole in the container as a guide, a hole was cut through the honeycomb with a sharp knife.

The sheathed thermocouple were hand bent to the drawing dimensions, and inserted up through the hole in the top plate and out the filler tube - bellows assembly. The thermocouple sheaths were held in place by forming stainless steel foil over the sheaths, and tack welding the foil to the sheaths and to the underside of the top plate. Five thermocouple junctions were positioned to monitor the vertical temperature gradient inside the container, at ~7 in. (177.8 mm) intervals. Three thermocouple junctions were located just below the top plate — one directly under the filler tube, the second near the concave surface of the container, and the third near the convex surface of the container. The latter two junctions were utilized to attain a symmetrical freezing pattern of the LiH toward the center of the container near the top.

The honeycomb matrix was lifted from the container, and held against the bottom of the top plate, while the thermocouple sheaths were inserted into the horizontal holes of the matrix. The matrix then was reinstalled in the container.

The penetration tube and the top plate were welded, and all weld joints dye penetrant checked and helium leak tested, to provide a leak-free vessel for the containment of the molten LiH during the casting cycle.

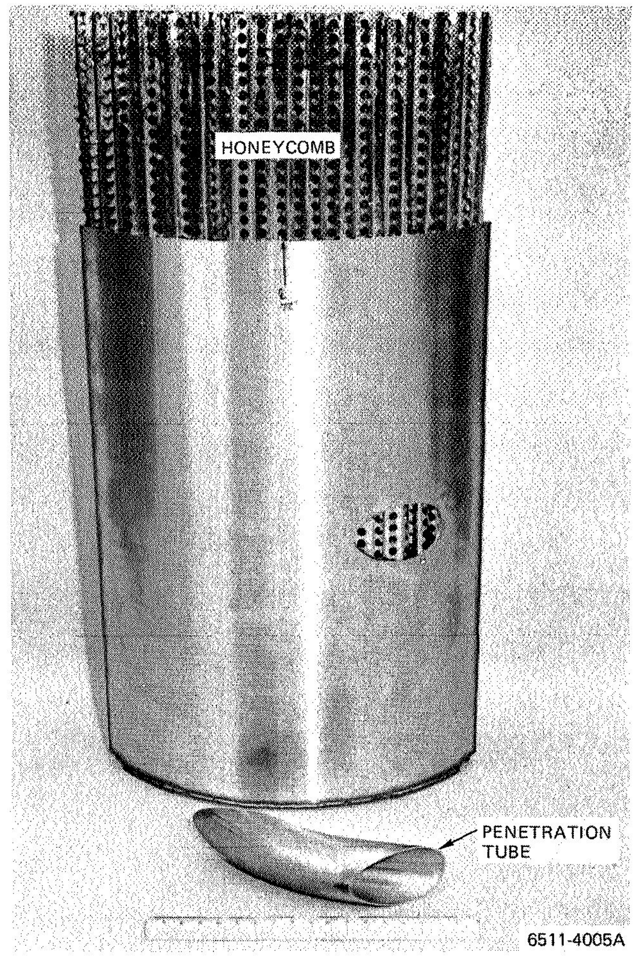

Figure 4.
Segment No. 7 During Assembly

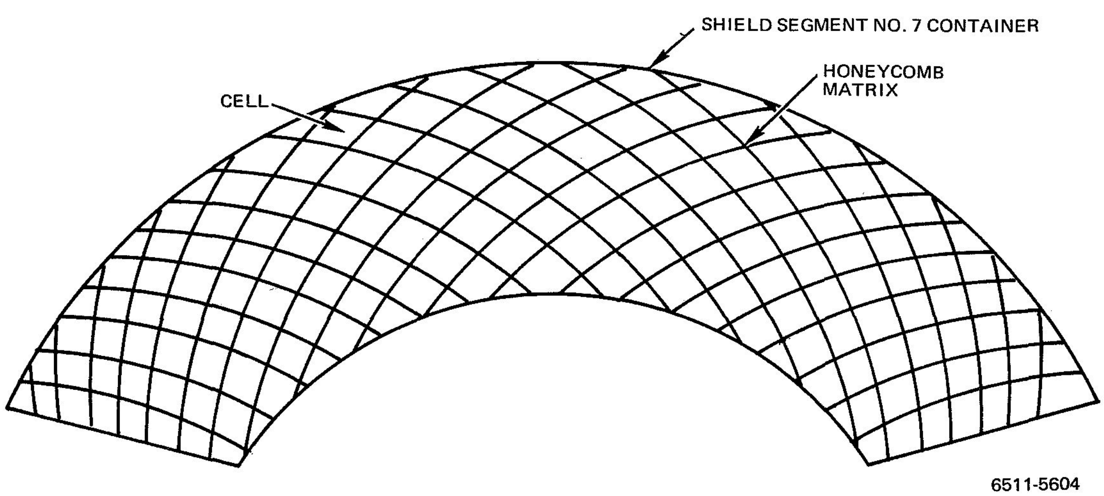

Figure 5. Top of Container, Looking Down at the Honeycomb

IV. PHASE I – TRIAL CASTING

In order to identify all potential problems, the most difficult segment was chosen for the trial casting. Segment No. 7 was selected for the following reasons:

1) The curved surfaces were the largest, and most likely to distort
2) The penetration tube was the largest, and most likely to interfere with the LiH freezing pattern
3) The top surface was the broadest, and most likely to exhibit gas pocketing on the underside.

The casting process consists of the following steps:

1) Assemble the shield container into the casting hardware
2) Load the LiH into the reservoir
3) Transfer the shield casting assembly to the retort base, and connect the thermocouples and trim heaters
4) Cover the assembly with the retort, seal, evacuate, and backfill with hydrogen gas (99.95% pure, minimum)
5) Install the bell furnace, and heat the retort and contents to ~1400°F (1033°K)
6) Raise the furnace from the retort, in preplanned increments, to establish a cooling gradient that permits the LiH to freeze in the shield from the bottom upward
7) Gradually adjust the furnace height, furnace temperature, and trim heater power until the LiH in the shield is completely solidified
8) Remove the furnace, and permit the shield assembly to cool to 300°F (422°K) or less
9) Evacuate the hydrogen from the retort, and backfill with argon gas
10) Unseal and remove the retort
11) Remove shield segment and casting hardware.

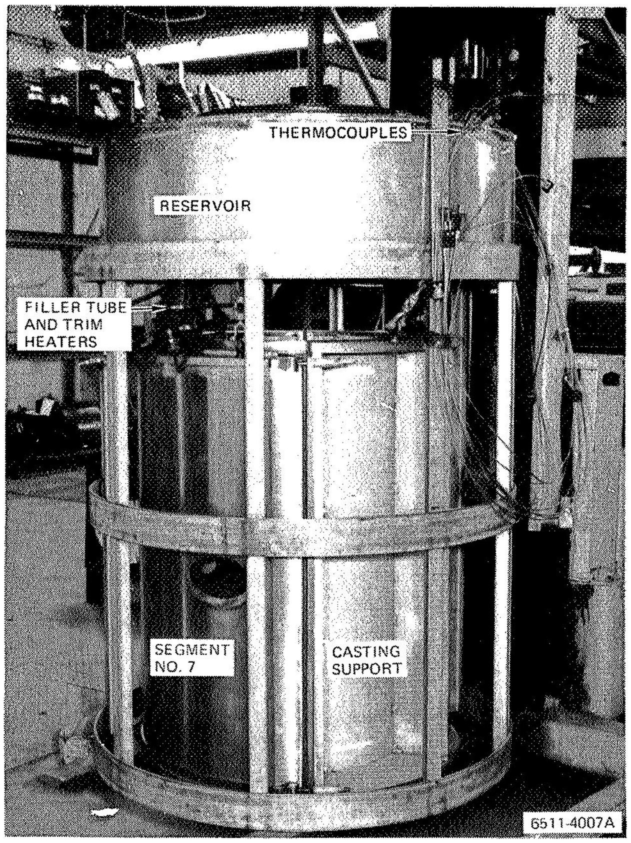

Figure 6.
Segment No. 7 in Casting Hardware

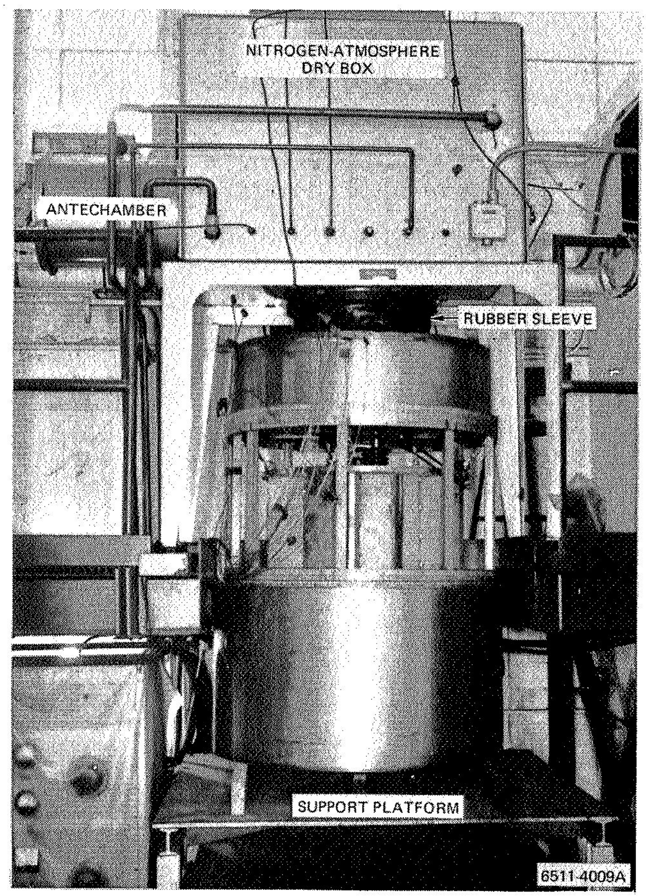

Figure 7.
Segment No. 7 Mated to LiH-Loading Dry Box

The following sections describe this process in detail for the trial casting, Segment No. 7.

A. ASSEMBLY

Segment No. 7 was installed in the casting fixture, the bands attached, and the casting hardware assembly completed with the welding of the filler tube - bellows assembly to the bottom of the reservoir. Figure 6 shows the completed assembly.

The assembly was moved onto the platform under the LiH-loading dry box, and mated with the dry box with a rubber sleeve (Figure 7). The air was purged from the dry box and segment with nitrogen gas until the oxygen content was reduced to 1 to 2%, as indicated on an oxygen analyzer which continually sampled the dry box atmosphere. Bags of granular LiH were weighed, moved into the antechamber, and the antechamber was purged of air. The LiH then was transferred into the dry box, and loaded into the reservoir. A total of 130 lb (58.96 kg) was loaded into the reservoir and segment.

The top of the reservoir was sealed with a gasketed lid, and the assembly removed from the platform. Twelve additional thermocouples were attached to the exterior surface of the segment and the casting support hardware, to monitor vertical and horizontal temperature gradients across the segment and the casting support.

The assembly was moved to the retort base, and the armored conductors attached to the trim heaters and the base terminals. High-temperature, fibrous, ceramic insulation was placed around all electrical connections in the high-temperature region, to prevent accidental grounding. The thermocouple plugs were mated with the retort base plugs. The gasketed lid was removed from the reservoir, and the retort placed over the assembly and bolted to the retort base. Figure 8 shows the completed assembly.

B. CASTING CYCLE

The retort was evacuated to 20×10^{-3} torr (2.67 N/m^2), at a rate of 10 to 15 torr/min (22 to 33 N/m^2-sec), to prevent "boilout" of the low-density LiH granules. The retort was filled with hydrogen (99.95% pure, minimum) to a pressure of ~850 torr (1133×10^2 N/m^2). The bell-type furnace, preheated to 600°F

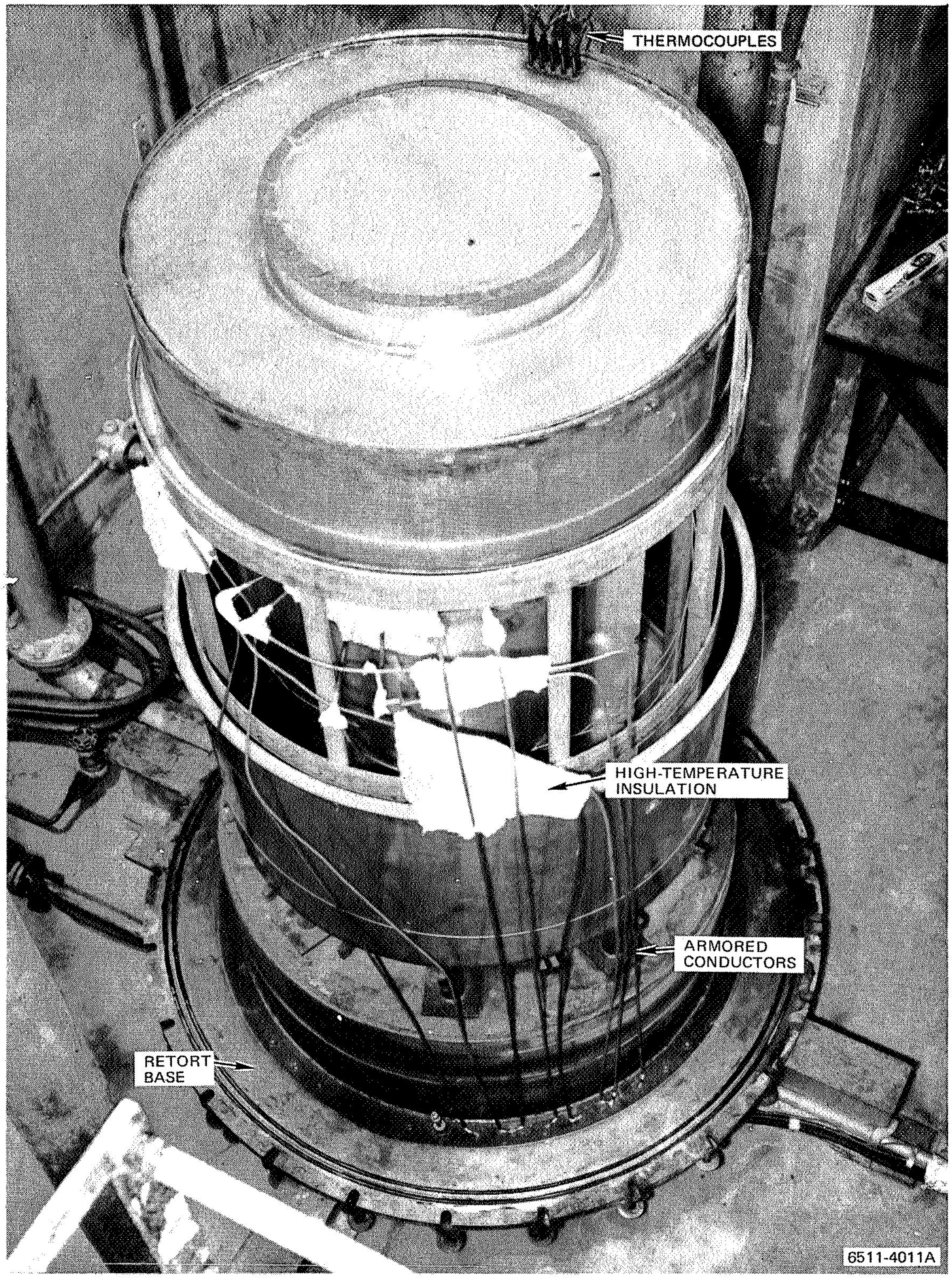

Figure 8. Segment No. 7 on Retort Base

(583°K), was lowered over the retort. The expanding hydrogen gas was vented and burned.

The retort and contents were heated beyond the 1267°F (959°K) melting point of the LiH, until all temperatures exceeded 1325°F (993°K). At this point, the hydrogen exhaust was closed, and the furnace raised 20 in. (0.508 m) to establish a thermal gradient in the segment, promoting freezing of the LiH from the bottom upward. The furnace thereafter was raised, in 2-in. (50.8-mm) increments every 2 hr, to maintain the gradient in the segment until a total lift of 40 in. (1.016 m) was reached. The furnace power and the reservoir trim heater power were adjusted to maintain the LiH in the reservoir above 1300°F (977°K) until the LiH in the segment was completely solidified.

After 5 hr of cooling, it was observed that two of the thermocouples [one, located 14 in. (355 mm) down from the top, along the side of the segment, and the other, located 0.75 in. (19 mm) down from the top, monitoring the gradient from the convex surface of the segment to the center] were indicating temperatures approximately equal to the temperature in the reservoir. Normally, these thermocouples should be indicating temperatures lower than the reservoir, because of the thermal gradient imposed upon the shield segment and the casting hardware by the cooling process. Manipulation of the furnace temperature, up and down, showed these thermocouples to respond rapidly; whereas, in a normal situation, these thermocouples should have been relatively insensitive to small changes in furnace temperature. Thus, it was suspected that these two thermocouples were malfunctioning.

The cooling cycle continued, without the ability to monitor the temperature differential between the inner and outer regions at the top of the segment, because of the thermocouple failure. (Note: Keeping the temperature differential small would cause inward symmetrical freezing of the LiH from the two sides toward the filler tube, resulting in a segment free of a casting void near the upper plate.)

A second problem encountered was the inability to maintain the reservoir at the desired temperature, using the reservoir trim heater. This problem was later diagnosed as excessive heat loss from the reservoir bottom to the retort base, through the open core of the support structure.

Examination of the temperatures of the twelve external thermocouples during the heating and cooling cycle indicated that the horizontal temperature gradients between the adaptor block and the segment, and the temperature gradients between the outside of the segment and the inside of the support structure, were <20°F (11.1°K). These small thermal gradients indicated that the casting support structure was not placing large thermal stresses on the segment during the cycle.

The casting cycle was terminated when all thermocouples, except the two noted as reading improperly, showed the LiH to be solidified. A total of 46 hr was required to complete the cycle.

When the LiH temperatures were near ambient, the retort was evacuated, backfilled with argon gas to atmospheric pressure, and the retort unsealed and removed.

Before the reservoir was sealed, it was observed that the two thermocouples, identified as malfunctioning, disappeared at the surface of the LiH in the reservoir, apparently having been dissolved by the LiH. It was later determined, by spectrographic analysis, that these two thermocouples were sheathed in Inconel 600 instead of Type 304 stainless steel. A third Inconel 600 sheathed thermocouple also was found in the lot of thermocouples procured for this contract. Inconel sheathing is not acceptable, since molten LiH is very corrosive to high-nickel-content alloys.

C. INSPECTION

An extensive program of nondestructive testing was established, to determine basic data on the segment and to provide the information upon which changes could be based, if required, to improve the characteristics of the Phase II production castings. X-ray radiography and void volume measurements were used to determine the integrity of the casting (i.e., the presence and size of voids and cracks). Dimensional measurements of the segment were used to establish the extent of distortion. Helium leak tests were used to establish the integrity of the container welds. Chemical and isotopic analyses were performed, to establish the purity and composition of the LiH.

1. Radiography

The segment was disengaged from the support structure, and a preliminary radiograph made before the segment was cut from the filler tube. A small void was observed in the region below, and to one side of, the filler tube (Figure 9). Additional radiographs were taken, to define the volume of the void. It was determined that the volume of the void was ~5 $in.^3$ (82 cm^3).

Final radiography, performed after the segment was severed from the filler tube, revealed the following additional information. Two agglomerations of cracks, 12 and 15 in. (305 and 381 mm) long, were located ~7 in. (17.8 cm) below the top plate. Also, a "chevron-shaped" crack (Figure 10), a part of the agglomeration, which appeared the most severe, was found to be a "double chevron." Each side was composed of two parallel cracks, ~1/16 in. (1.6 mm) wide, with a depth between 3/8 and 1 in. (9.5 and 25.4 mm). These cracks were determined to be ~1/8 in. (3.2 mm) apart, and located ~1 to 2 in. (2.54 to 5.08 cm) from the convex side of the segment. Appendix 3 describes the parallax technique used to determine the crack dimensions.

Penetrameters of beryllium metal, which has an electron density near that of LiH, were used to determine the radiographic sensitivity. A 0.060 in. (1.52 mm) beryllium disc was clad with 0.001-in. (0.0254-mm) thick stainless steel foil to simulate the LiH-filled container. A 0.120-in. (3.04-mm) thick disc of unclad beryllium was also made.

Examination of radiographs made with the penetrameters attached to the segment revealed that the thinnest disc (1% of the total thickness of the segment) was barely visible, whereas the thicker disc (2% penetrameter) was clearly visible. The radiographic sensitivity was judged to be ~2%.

Holes, 0.060 in. (1.52 mm), 0.120 in. (3.05 mm), 0.240 in. (6.10 mm) and 0.480 in. (12.19 mm) in diameter, were drilled through the beryllium metal to determine the defect sensitivity. Examination of the radiographs showed that the smallest hole was visible.

2. Void Volume

The void volume of the segment was determined by evacuating the segment and then backfilling the segment with argon to atmospheric pressure from a tank

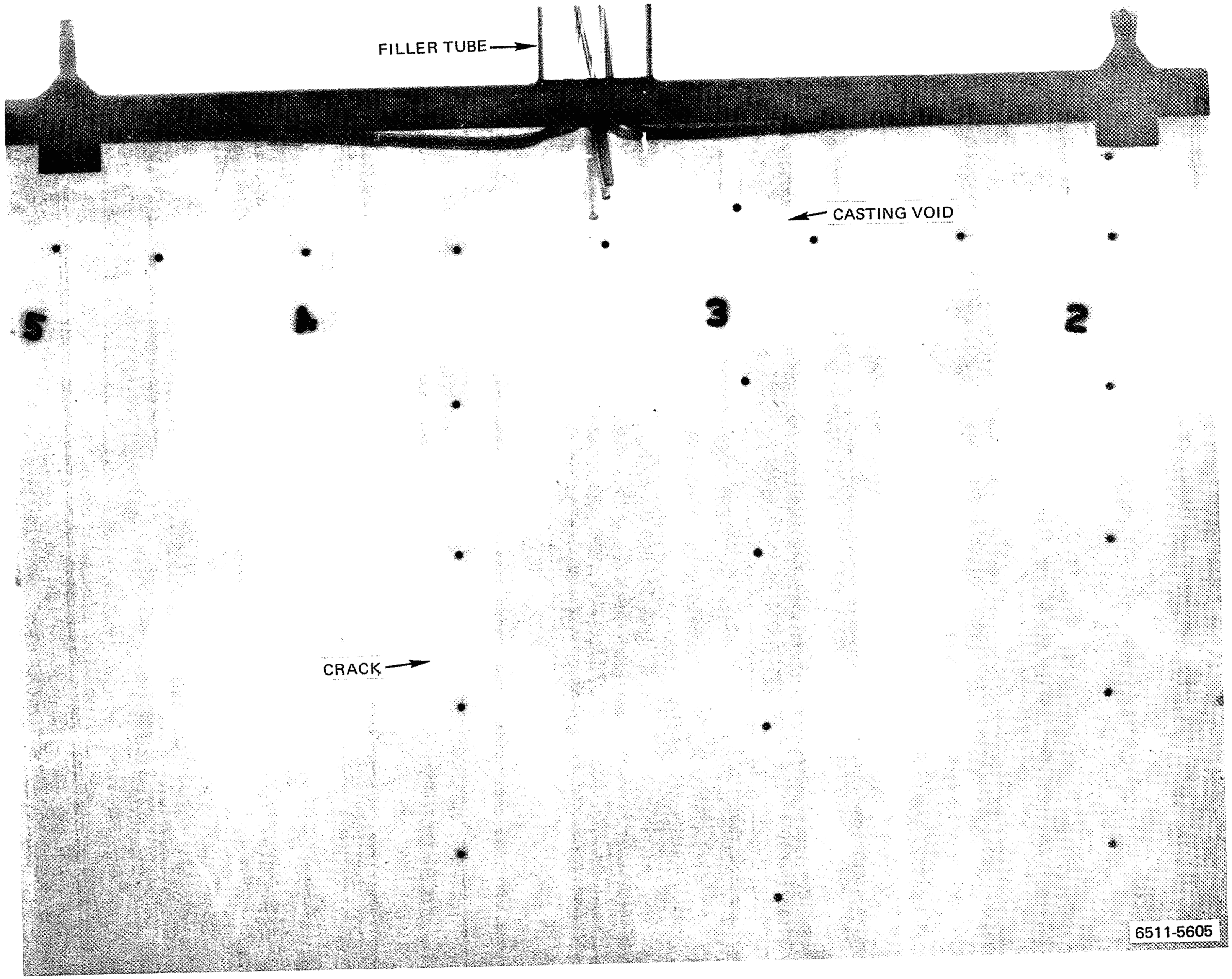

Figure 9. Segment No. 7 Preliminary Radiograph

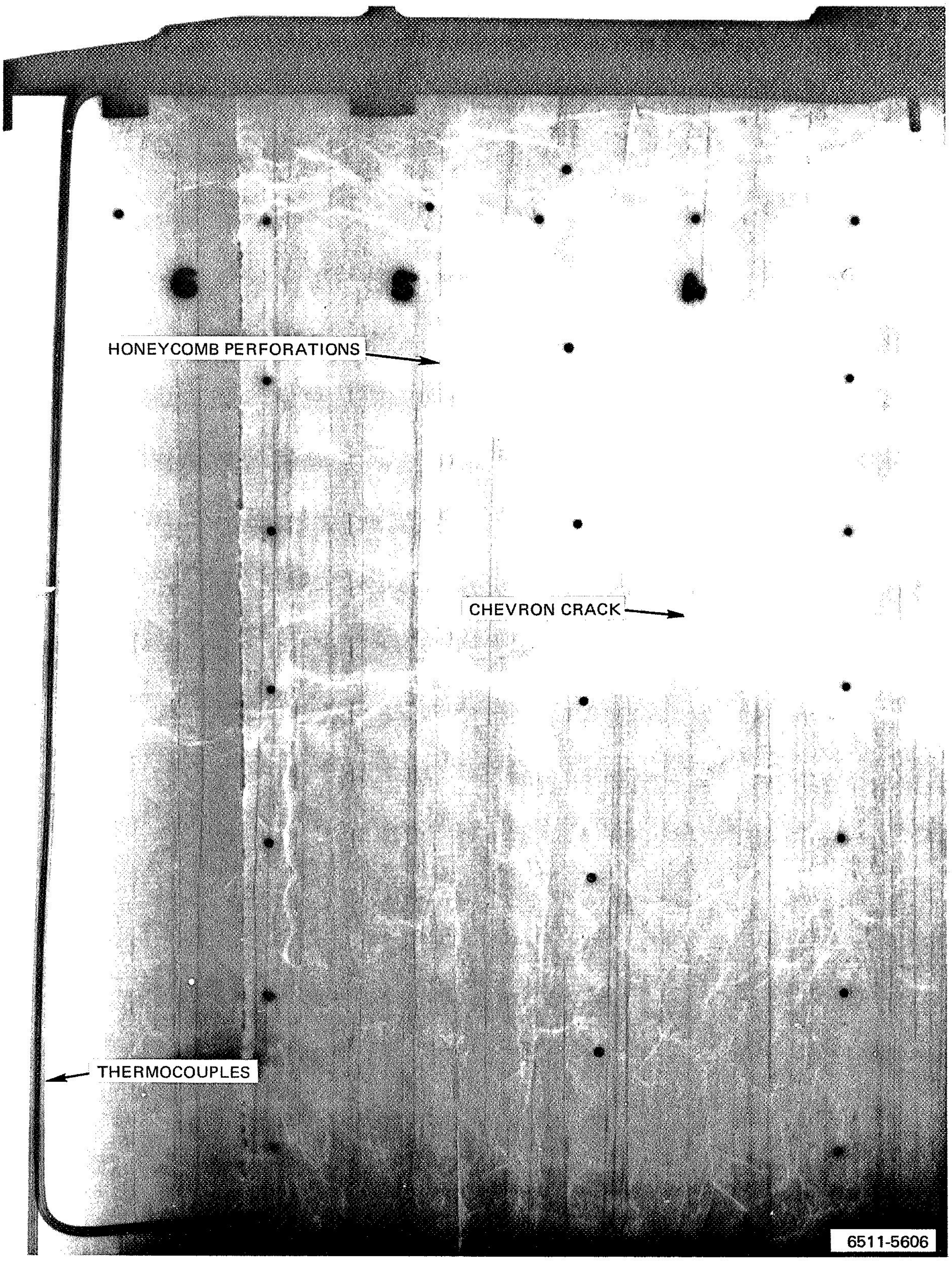

Figure 10. Segment No. 7 Final Radiograph

of known volume and pressure. The void volume was determined to be 6.5% which is equivalent to a casting with a theoretical density of 93.5%. The program requirement was 93% minimum.

3. Dimensional Inspection

The segment was placed on an inspection surface plate, and the normality of the segment measured at eight locations on the surface (three positions on the convex and concave surfaces, and one position on each side plate). These measurements (see Appendix 5) showed that the sides of the segment were not normal to the base, and that the segment had a twist over its length, from top to bottom, such that one corner of the top plate was 0.080 in. (2.03 mm) out of perpendicular with the base. Figure 11 schematically illustrates the twist of the segment. Since detailed precast dimensional data were not available, it was not possible to separate the casting-cycle-produced distortions from the fabrication-induced distortions.

A detailed dimensional inspection of the casting support fixture revealed that the base plate was not perpendicular to the vertical cylinder, but was sloped, 0.080 to 0.090 in. (2.03 to 2.29 mm), across the cavity in which the container was confined. The outer edge of the base plate also was found to be slightly higher than the inner edge. The action of the segment, restrained in the "cocked" configuration by the bands during the casting cycle, would be to yield into a "twisted" shape, as noted. Subsequent experience with the production castings indicated the twist probably was introduced during casting, by the out-of-perpendicular casting support fixture.

4. Helium Leak Check

Prior to casting, the empty container was helium leak checked, using an internal pressure of 0.3 psig (2×10^3 N/m^2) of helium. After casting, the LiH-filled segment was helium leak checked in the evacuated condition with a helium gas probe on the external surface. During final closure, the segment was evacuated, backfilled with helium, and the closure cap welded into place. This final weld joint was checked by the evacuation method. The leak rate was found, in all cases, to be $<1 \times 10^{-9}$ STD cm^3/sec of helium.

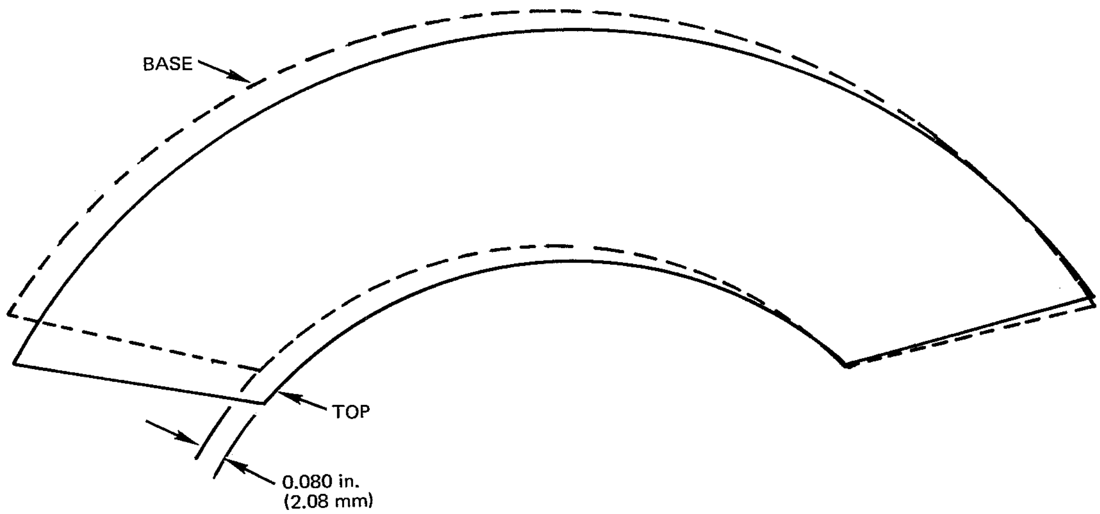

Figure 11. "Twist" Found in Segment No. 7

TABLE 1

CHEMICAL ANALYSIS OF LiH FOR SEGMENT No. 7

	Specification	Precast	Postcast	Precision
LiH (wt %)	97.5 minimum	99.7	96.6 est.	±1.0
OH (wt %)	1.5 maximum	1.30	2.21	±0.2
CO_3 (wt %)	1.0 maximum	0.03	0.07	±0.02
Cl (wt %)	0.1 maximum	0.04	0.01	±0.01
Na (ppm)	300 maximum	50	95	±10%
K (ppm)	400 maximum	50	62	±10%
Co (ppm)	60 maximum	50	50	±10%

5. LiH Chemical Analysis

Samples of LiH were removed from each bag used for Segment No. 7. These samples were composited, and three samples were removed from the composite for analysis. After casting, a sample of LiH was removed from the filler tube for analysis. Table 1 compares the results of these analyses and the specification values.

As may be seen in Table 1, the precast percentage of LiH is quite high, giving a total for all components to be >100%. The analysis of LiH was by thermal decomposition. Although the precision or repeatability of the group of measurements is ±1.0, the accuracy or true value cannot be determined, since standards for the LiH analysis are not available. In the postcasting chemical analysis, the LiH content was not measured. The value shown was determined by subtracting the total of all other components from 100%.

The high value for the postcast OH content, 2.21%, was attributed to the presence of the casting void, and the consequent concentration of impurities near the top of the segment. Normally, during the casting cycle, a refining process occurs, whereby the impurities are lifted out of the container, up into the filler tube, and are finally frozen out near the top of the filler tube or in the reservoir. When this process is interrupted (i.e., the supply of molten LiH from above is cut off), the trapped LiH will contain a higher-than normal amount of impurities, which will remain in the segment or the lower portion of the filler tube. This action was confirmed by an analysis of another sample of LiH, removed from below the top plate of Segment No. 7, where the void was located. This sample contained 2.67 wt % OH, and only 94.97 wt % LiH. High concentrations of unspecified elements (Cr, Fe, and Ni) also were found in this sample, and were attributed to the dissolution of the Inconel 600 thermocouple sheath. The presence of the high concentration of impurities in the filler tube sample of LiH also was attributed to the dissolution of the thermocouple.

D. PHASE I DISCUSSION

While the trial casting proved the feasibility of casting the desired shape, several problems were revealed, which were evaluated in detail prior to initiation of the production casting phase.

Although cracks were observed in the LiH, the presence of the stainless steel honeycomb matrix successfully prevented the propagation of the cracks, and kept the crack width and depth to acceptable sizes. However, evaluation of the radiographs of the trial casting was complicated by the lack of a representative standard, in terms of a known defect in a block of cast LiH. Therefore, in an attempt to improve the resolution of size and depth of cracks, a slot was added to the top plate of the next segment to be cast. This slot was used as a guide to drill a cavity, 1/8 in. (3.18 mm) wide by 2 in. (50.8 mm) long by 1 in. (25.4 mm) deep, into the cast LiH, which could be used in the radiographic examination as a known size for comparison purposes.

The presence of the casting void, although within specification limits, was undesirable. Also, this type of defect tends to produce a chemical purity problem. It appeared that the void in Segment No. 7 was caused by "off-center" freezing, which was not detected because of the loss of the Inconel-sheathed thermocouples. Additional thermocouples were added in this region for the production castings, to provide for additional monitoring of local temperatures below the filler tube. It was believed that these thermocouples, and the use of the filler tube trim heaters, should prevent the void formation below the filler tube.

The loss of these critical thermocouples, because of the accidental introduction by the vendor of sheathing material with no resistance to molten LiH corrosion, points up the necessity of in-house verification of all materials which will be in contact with molten LiH.

The out-of-normality of the segment, and the twist of the top plate in relation to the bottom plate, represented a potential problem. These discrepancies could, if compounded with similar discrepancies in other segments, introduce interference with the remainder of the shield test assembly. Therefore, welded pads or shims were installed on the casting support cavity, and a precise technique defined to align future segments with the vertical cylinder. This modification was subsequently shown to eliminate the twist problem.

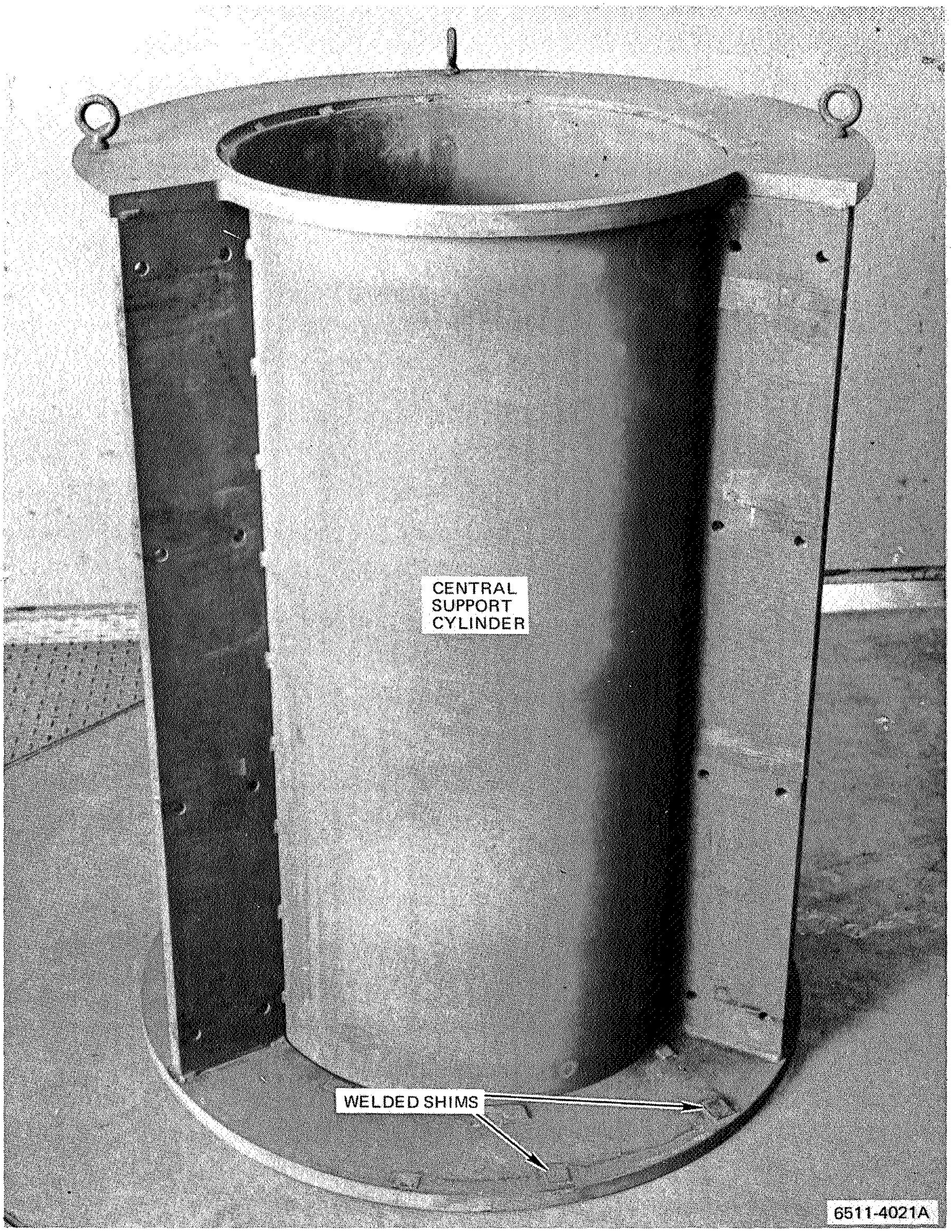

Figure 12. Casting Fixture With Shims

V. PHASE II – PRODUCTION CASTINGS

The second phase of the program provided for the fabrication, casting, and nondestructive testing of the shield segments, based upon the information gained from the trial casting. Although the trial casting (Segment No. 7) was moderately distorted, it could be usable, if the distortions of the remaining three segments (No. 1, 2, and 3) were better controlled. Thus, the order of casting in Phase II was established as Segments No. 3, 2, 1, and lastly No 7, if necessary.

A. CONTAINER FABRICATION

The production containers were built in the same manner as the trial casting container, except that three thermocouples were added inside the container (below the top plate, near the filler tube), to provide additional temperature monitoring in the region where the casting void occurred. Also, the Segment No. 3 top plate was modified, to provide the slot (temporarily covered with a welded stainless steel plate during the casting) which could be used as a guide to drill a slot in the LiH for radiographic comparison use.

During the precast contour dimensional inspection of these containers, it was found that the containers were not normal to their bases. Welded shims were added to each container to improve the normality. Appendixes 6 to 8 show the precast normality values of the containers after shimming.

B. ASSEMBLY

Stainless steel shims were welded to the baseplate of the casting support fixture, and filed until all contact points formed a plane that was perpendicular to the fixture centerline within ±0.002 in. (0.05 mm) (Figure 12). This accomplished the alignment of the shield segment centerline with the fixture centerline.

The casting assembly was completed in the same manner as described for Segment No. 7, except that the high-temperature, fibrous, ceramic insulation also was placed on the underside of the reservoir to reduce the heat loss. Since these segments were smaller than Segment No. 7, only 100 lb of LiH were required for each casting.

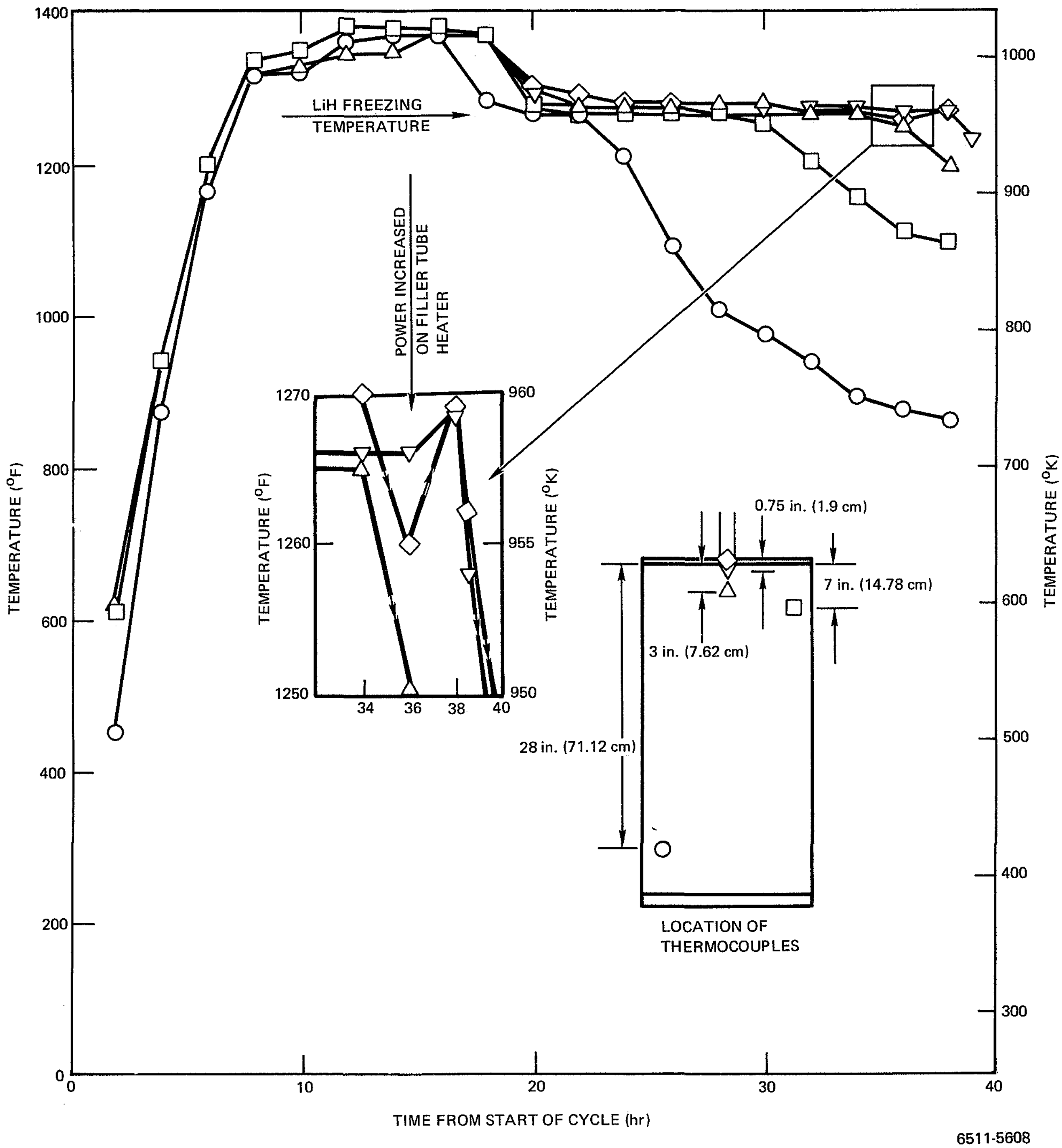

Figure 13. Segment No. 2 Casting Cycle

C. CASTING CYCLE

The casting cycle for all segments in Phase II proceeded without incident, but for one exception. A small casting void was found at the top of the Segment No. 3 (the first of the production segments). Evaluation of the reasons for this occurrence led to the conclusion that excessive heat loss from the thick top plate was causing the LiH to freeze, and bridge across the opening in the top plate, leaving a small pocket of molten LiH below the bridge to freeze out later and create a void (LiH decreases in volume, by ~20%, upon freezing). As a corrective measure for the remaining segments, a 1/2-in. (12.75-mm) thick copper plate was placed on the top plate, around the filler tube, to more evenly distribute the heat. In addition, a thermocouple was inserted down the filler tube, with its junction located at the level of the top plate, to detect the occurrence of the premature freezing.

During the cooling cycle for both Segments No. 2 and No. 1, as the freezing zone progressed to the top of the segment, the new thermocouple was observed to take a slight drop in temperature, indicating that the LiH was freezing at the top plate, but was still molten higher up in the filler tube and in the segment just below the top plate. The power to the filler tube trim heaters was increased slightly, to keep the LiH molten at the top plate. The cooling cycle then continued in a normal progression of freezing. This procedure solved the filler tube void problem. Figure 13 shows the heating and cooling cycle for Segment No. 2, illustrating the sharp drop in temperature at the top plate, and the recovery after power to the filler tube trim heaters was increased.

No problem was encountered with heat loss from the reservoir, after the addition of the insulation to the underside.

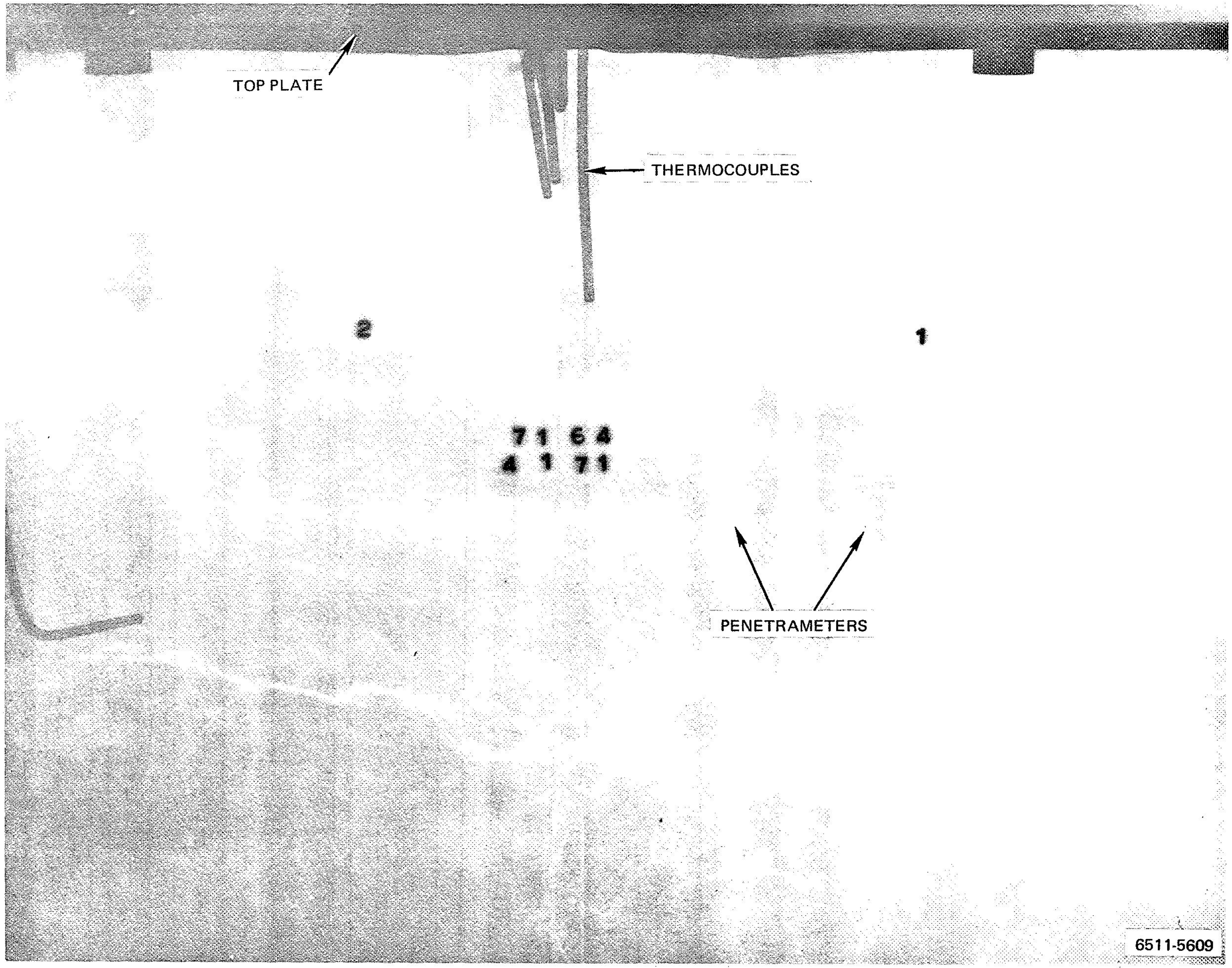

Figure 14. Segment No. 2 Radiograph at Top

VI. RESULTS AND DISCUSSION OF RESULTS

A. INSPECTION

1. Radiography

Radiographic examination of Segment No. 3 revealed the casting void to have a volume of 3-1/8 in.^{3} (51.2 cm^3), and to be located approximately in the same position below the filler tube as the void found in Segment No. 7 (Figure 9). An agglomeration of cracks was observed ~20-3/4 in. (52.7 cm) down from the top plate, exceeding the 8 in. (20.3 cm) crack length allowed by the specification. These cracks were determined to be ~1/2 in. (1.27 cm) deep and 0.1 in. (2.5 mm) wide.

The slot drilled in the LiH was determined to be 2.4 in. (6.1 cm) long, using the parallax technique. Because the actual length of the slot was 2.0 in. (5.08 cm), it appears that the parallax technique results in a crack length determination 20% greater than actual.

Radiography indicated Segments No. 1 and 2 to be free of casting voids. Figure 14 shows the view at the top of the Segment No. 2. Cracks were visible between the LiH crystals, as is normal for the cast material, although no cracks were out of specification. These cracks were 1/8 to 1/16 in. (3.1 to 1.6 mm) wide, 1/2 in. (1.27 cm) deep, and 1 to 6-3/4 in. (2.54 to 17.1 cm) long.

2. Dimensional Measurements

Pre- and postcasting dimensional measurements on Segments No. 1, 2, and 3 showed that the technique of shimming essentially eliminated the twist found in the trial casting. The greatest changes in dimensions of the segments after casting was a pull-in of the surfaces, producing a concavity which would not create a fit-up problem in the assembly. Appendices 6 to 8 show these dimensions for the three segments.

The improvement in the control of distortions in Segments No. 1, 2, and 3 that affected the fit-up of the segments into an annulus permitted the use of the trial casting as Segment No. 7. Thus, it was not necessary to cast another Segment No. 7 in Phase II.

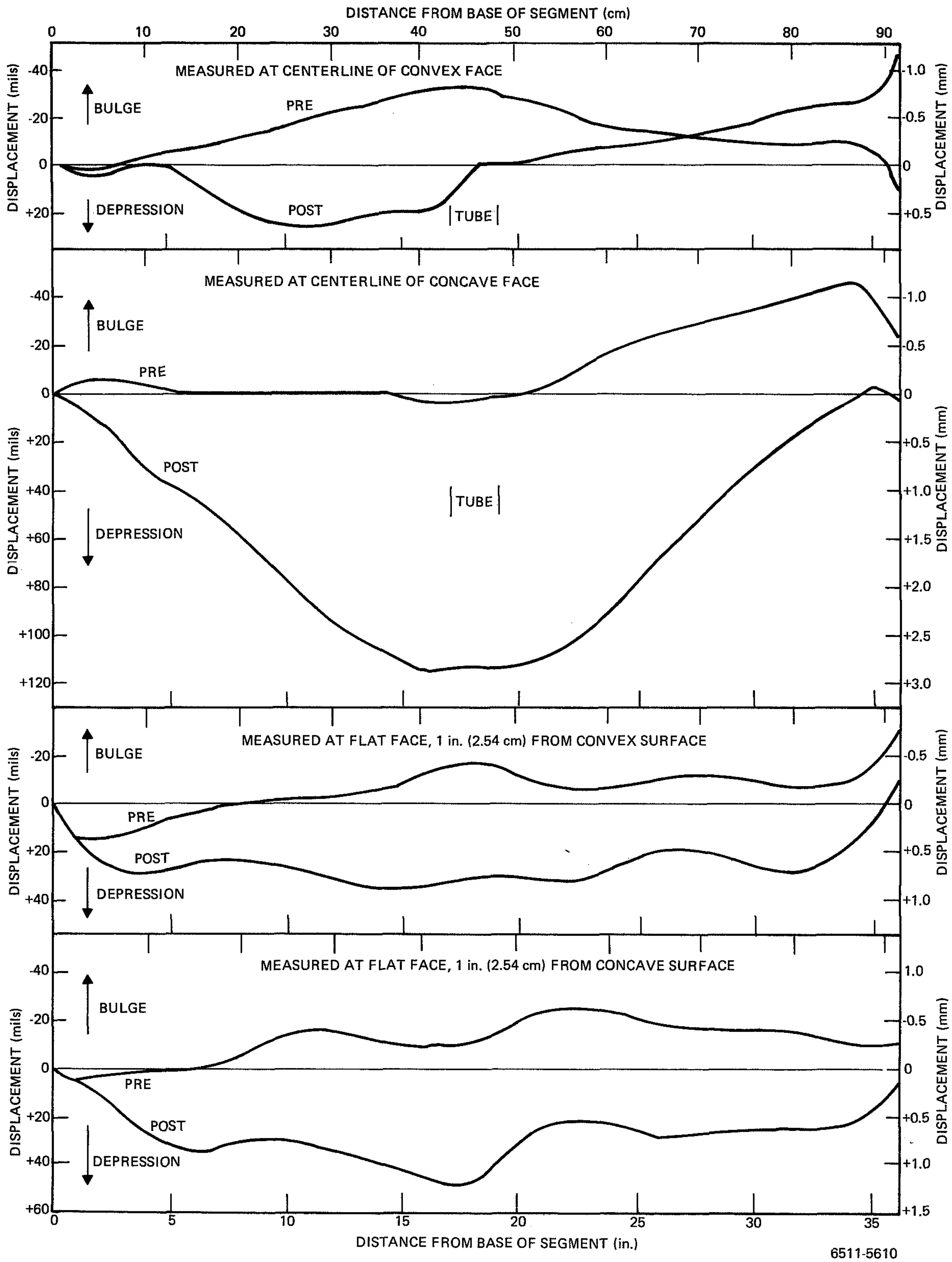

Figure 15. Pre- and Postcasting Profiles of Segment No. 1

Figure 15 illustrates the changes in dimensions of Segment No. 1 caused by the casting cycle. The unrestrained convex face did not distort outward significantly at the centerline profile, shown in Figure 15. However, at Position C (see Appendix 6) and Position B (see Appendix 7), the convex faces on Segments No. 1 and 2, respectively, bulged outward a maximum of 0.043 in. (1.09 mm) from the as-fabricated position, due to the casting cycle.

All of the concave faces and the side plates of the segments cast in Phase II were drawn inward, producing a concavity. The concave face of Segment No. 1 at the centerline pulled inward ~0.116 in. (2.94 mm), due to the casting cycle, as shown in Figure 15. This was the maximum pull in of all segments that were cast in Phase II. Figure 15 also shows that the concave faces and the side plates had the same general profile after casting as they had before casting. This characteristic manifested itself on all three shield segments cast in Phase II.

3. Helium Leak Check

All segments were helium leak checked, and no leaks >1 x 10^{-8} STD cm^3/sec of helium were found at a pressure differential of 1 atm (1.013 x 10^5 N/m^2).

B. VOID-VOLUME RESULTS

The void volume of the production segments was measured in the same manner as described for the trial casting. Table 2 shows the results of all measurements, and the calculated weight of LiH in each segment.

C. CHEMICAL AND ISOTOPIC ANALYSES

Prior to the casting of the three production segments, all bags of LiH were sampled, composited, and analyzed. After each casting, a sample of LiH was taken from the filler tube for analysis. Table 3 shows the results. Six samples of LiH from a composite of the original bags of LiH were analyzed for Li^6 isotopic content. The Li^6 abundance was found to be 7.49 at.%. The precision was ±0.07%, and the accuracy was ±0.05%. The confidence interval was 95%. The specified value was 7.42 ± 0.2 at.%.

The amount of LiH in the three postcasting analyses, although not determined, can be estimated, from the percentages of the other components, to be >98%. In general, the percentages of all impurities were slightly higher in the samples removed from the filler tube, as compared to the precast composition.

TABLE 2

VOID VOLUME OF SHIELD SEGMENTS

Segment No.	Void Volume (%)	Percent of Theoretical Density	Calculated Weight of LiH/Segment	
			(lb)	(kg)
1	5.8	94.2	84.7	38.5
2	5.9	94.1	85.1	38.7
3	6.1	93.9	81.2	36.9
7	6.4	93.6	100.5	159.8
Total			351.5	159.8

TABLE 3

CHEMICAL ANALYSIS OF LiH FOR PRODUCTION SEGMENTS

	Specification	Precast*	Postcast			Precision
			No. 1	No. 2	No. 3	
LiH (wt %)	97.5 minimum	98.6	ND	ND	ND	±1.0
OH (wt %)	1.5 maximum	0.47	0.74	0.83	0.51	±0.2
CO_3 (wt %)	1.0 maximum	0.06	0.057	0.095	0.06	±0.02
Cl (wt %)	0.1 maximum	<0.01	0.018	0.012	0.01	±0.01
Na (ppm)	300 maximum	31	25	100	15	±10%
K (ppm)	400 maximum	48	5	<25	<5	±10%
Co (ppm)	60 maximum	<50	50	<50	<50	±10%

*Average of three composites, two analyses of each composite
ND = not determined

This is to be anticipated, since, as described earlier, the casting process has a refining action, lifting the impurities from the segment, mainly into the reservoir, and to a lesser extent into the filler tube.

The slightly increased OH content probably is partially due to the refining action, and partially due to the increased handling of the sample during the cutting off of the filler tube, the removal of the LiH sample in the nitrogen-atmosphere dry box, and the subsequent handling during chemical analysis. All of these actions introduce the possibility of some slight exposure of the LiH to water vapor, creating the lithium hydroxide (LiOH) impurity.

D. FINAL HARDWARE

Figures 16a and b show the four completed segments, and Figure 17 shows the four segments assembled into a cylinder.

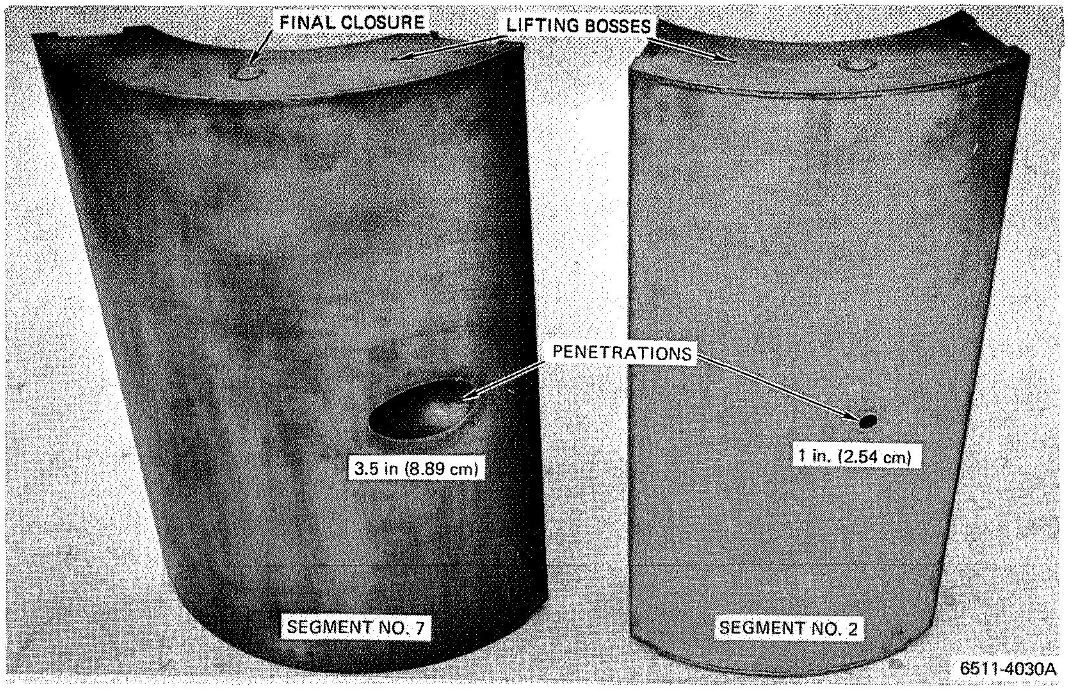

a. Segments 2 and 7

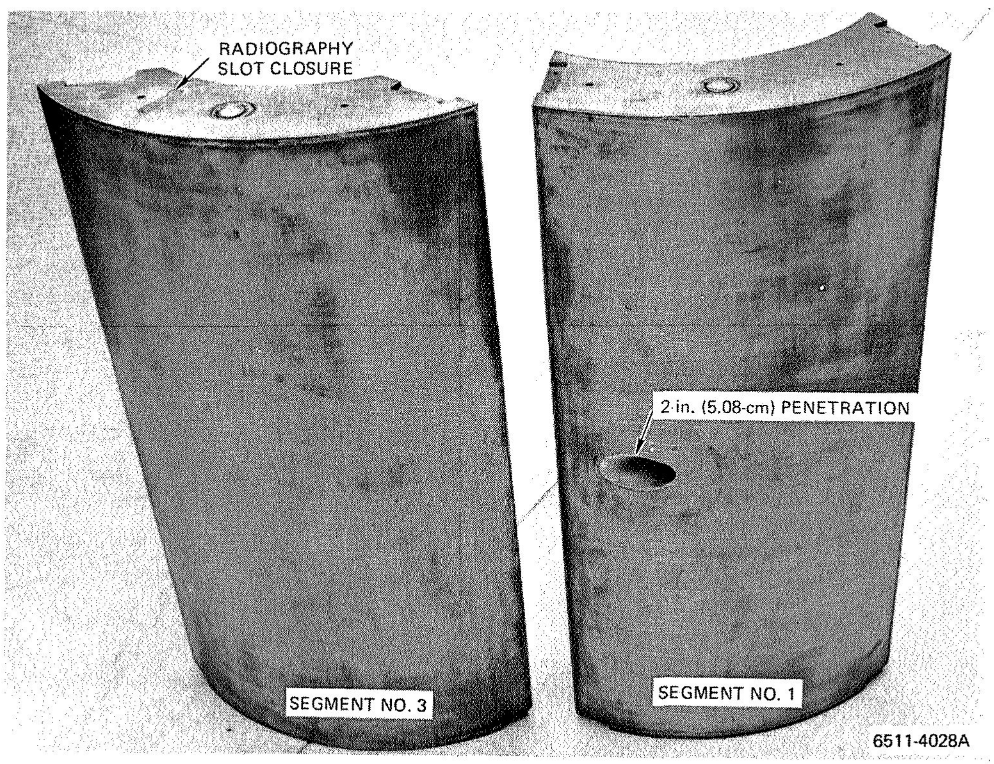

b. Segments 1 and 3

Figure 16. Production Segments

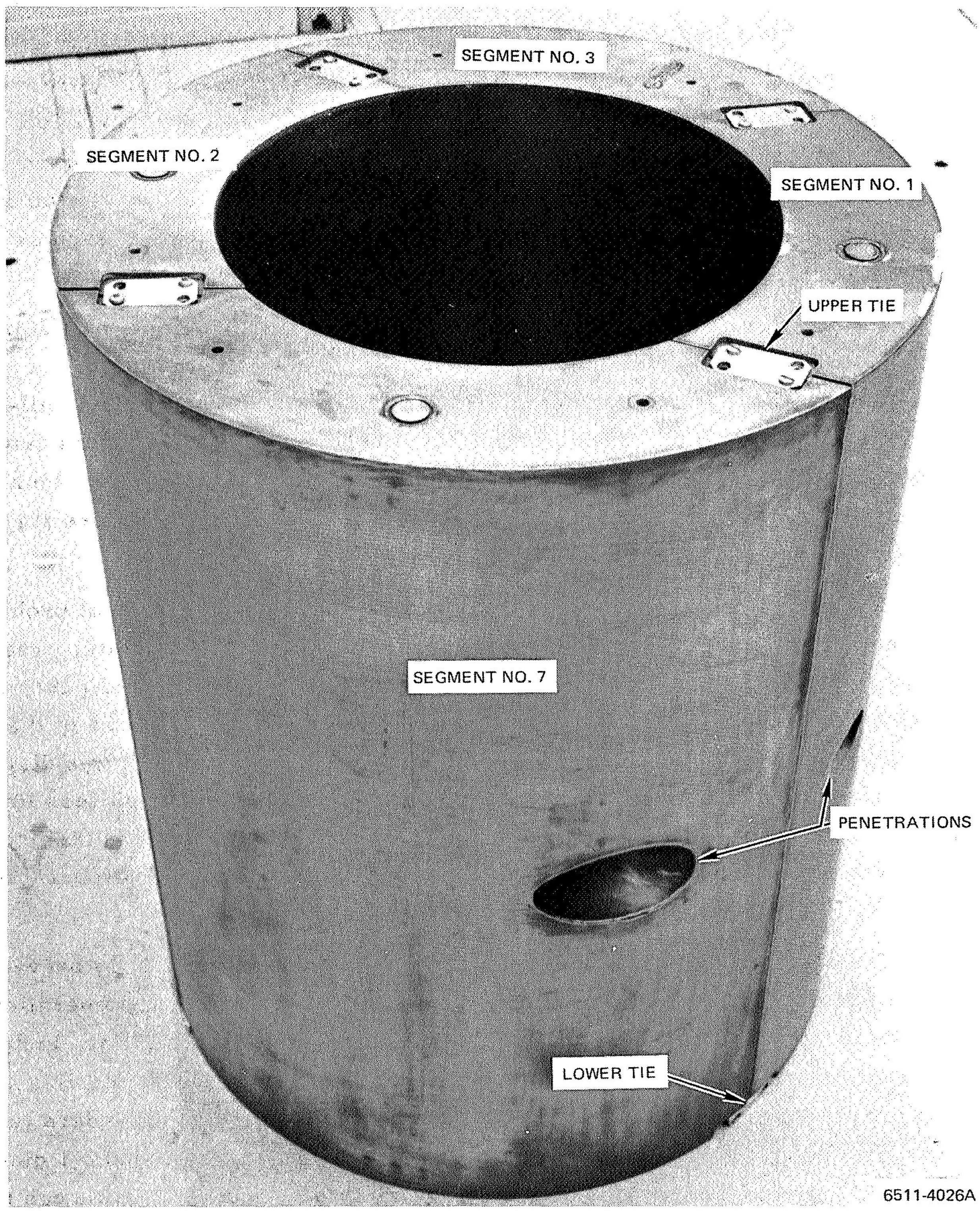

Figure 17. Assembled Segments

VII. CONCLUDING REMARKS

Four shield segments that formed a right cylindrical annulus were designed, fabricated, and filled with natural lithium hydride by casting into welded, stainless steel containers. The unique shape and construction of these shield segments introduced problems not previously encountered in LiH shield fabrication, which had been limited to the fabrication of symmetrical shapes, such as cones or cylinders.

The annular cylinder sector geometry exaggerates problems of distortion, not only during the fabrication of the container, but during the thermal cycle of the casting process. These distortions generally were found to be a pull-in of the sides, caused by the contracting LiH. This type of distortion was anticipated, but the magnitude was not known. Elimination of these distortions in flat surface geometries may be difficult, requiring, for example, a more rigid design of the flat surface.

The thick top plate in the shield segments introduced a potential problem of excessive heat loss and a premature freezing of the LiH at the plate, creating a casting void. The problem was easily corrected by the addition of a thermocouple at the critical point, and slightly increasing the temperature of the LiH in the filler tube and at the top plate, once the cause of the problem was diagnosed. In future geometries, where thick sections may cause excess heat loss in the filler tube region, care must be taken to provide thermocouples in the proper locations to detect such losses, and trim heaters to control the temperature of the LiH.

The internal honeycomb was effective, in these geometries, in preventing excessive propagation of individual cracks. However, some agglomeration of cracks in cast LiH was noted in each shield. The highly crystalline, brittle material apparently cracks from the stresses induced during the cooling of the solidified LiH. The author previously has observed that long cylinders tend to crack horizontally, in a recurring pattern, with the cracks spaced ~ 1 diameter apart. A similar recurring pattern appeared in these castings, although the presence of the penetrations tended to disrupt the regularity.

Improvement in the detection and precise location of cracks in the LiH is seriously needed, since there is no easy solution to their elimination. The present method, using the parallax technique, is an approximation, and cannot fully define the type and geometry of the cracks.

REFERENCES

1. F. H. Welch, "Lithium Hydride Technology — Fabrication of Shadow Shields for SNAP Applications," NAA-SR-9400, Vol II (September 30, 1965)

2. F. H. Welch, "Space Reactor Shielding Fabrication," National Symposium on Natural and Manmade Radiation in Space, March 1, 1971 (to be published as a NASA-SP Proceedings)

APPENDICES

APPENDIX 1

LIST OF DRAWINGS

1. "Segment No. 7 — Lithium Hydride Shield," A.I. Dwg. N00123007 (NASA Dwg. CF352254)
2. "Segment No. 3 — Lithium Hydride Shield," A.I. Dwg. N00123009 (NASA Dwg. CF352252)
3. "Segment No. 2 — Lithium Hydride Shield," A.I. Dwg. N00123008 (NASA Dwg. CF352251)
4. "Segment No. 1 — Lithium Hydride Shield," A.I. Dwg. N00123010 (NASA Dwg. CF352251)
5. "Lower Tie — Lithium Hydride Shield," A.I. Dwg. N00123012 (NASA Dwg. CF352254)
6. "Upper Tie — Lithium Hydride Shield," A.I. Dwg. N00123013 (NASA Dwg. CF352254)
7. "Casting Support Assembly — Lithium Hydride Shield," A.I. Dwg. EX-N00123015)
8. "Adaptor Blocks — Casting Support — Lithium Hydride Shield," A.I. Dwg. EX-N00123016
9. "Bands and Nut — Casting Support — Lithium Hydride Shield," A.I. Dwg. EX-N00123026
10. "Safety Container — Lithium Hydride Shield," A.I. Dwg. EX-N00123018
11. "Support Structure — Lithium Hydride Shield," A.I. Dwg. EX-N00123019
12. "Reservoir — Lithium Hydride Shield," A.I. Dwg. EX-N00123020
13. "Lid — Lithium Hydride Shield," A.I. Dwg. EX-N00123021
14. "Lug — Lithium Hydride Shield," A.I. Dwg. EX-N00123022
15. "Bellows Assembly — Lithium Hydride Shield," A.I. Dwg. N00123006
16. "Bellows Heater — Lithium Hydride Shield," A.I. Dwg. EX-N00123023
17. "Reservoir Heater — Lithium Hydride Shield," A.I. Dwg. EX-N00123024
18. "Core Heater — Lithium Hydride Shield," A.I. Dwg. EX-N00123025
19. "Thermocouple — Type K — Lithium Hydride Shield," A.I. Dwg. N00123011
20. "Casting Support Assembly — Lithium Hydride Shield," A.I. Dwg. EX-N00123017

APPENDIX 2

SPECIFICATION FOR LITHIUM HYDRIDE SHIELDS

A. Scope — This specification covers the requirements for cast lithium hydride for the Zero Power Reactor (ZPR) shield experiment which will be conducted at the NASA-Lewis Research Center.

B. Description — The lithium hydride shield is an annular cylinder consisting of four sectors. The operating temperature of the shield will not exceed 100°F. The shield will either be immersed in water or be in a high humidity atmosphere.

C. Materials — The contractor shall provide all materials used for fabricating the lithium hydride shields. These materials shall conform to the following requirements:

1. Lithium Hydride:

   a. Isotopic Content — The lithium hydride shall contain natural lithium. The average lithium-6 content shall be 7.42 ± 0.20 atom percent and shall be known to within ± 3 percent relative to the 95 percent confidence level.

   b. Lithium Hydride Composition — The lithium hydride material shall contain not less than 97.5 percent (weight) of lithium hydride. The impurities shall not exceed the following amounts:

Hydroxide (OH)	1.5 wt %
Carbonate (CO_3)	1.0 wt %
Chloride (Cl)	0.1 wt %
Sodium (Na)	300 ppm
Potassium (K)	400 ppm
Cobalt (Co)	60 ppm

2. Container and reinforcing material — The container and reinforcing (honeycomb) material shall be an austenitic stainless steel (300 series). Type 304 or 316 stainless steel is recommended for their good welding characteristics.

D. Requirements of Lithium Hydride-Container Assemblies — The lithium hydride shall be cast directly into the stainless steel containers.

1. Lithium hydride density — The lithium hydride density as cast in the container shall be 93 percent or greater of theoretical density.

   a. Voids — In the vicinity of the filler tubes only, a maximum void cavity of ten (10) cubic inches is permissible. These voids shall not extend more than three (3) inches in any direction from the center of the filler tube. Void cavities in the cast lithium hydride other than those near the filler tubes and cracks (see below) are not permissible.

b. Cracks — The amount and sizes of cracks in the cast lithium hydride shall be minimized within the present "state-of-the-art" casting technology. The maximum crack size shall be 8 inches long, 1/8-inch wide, and 3 inches deep in areas away from the tubular penetrations. Honeycomb reinforcement shall be used to limit the sizes of cracks (see section D-3 below). The honeycomb shall be installed in a manner such that radial cracks do not extend more than 1/3 (2 inches) into the thickness of the lithium hydride shield (see sketch).

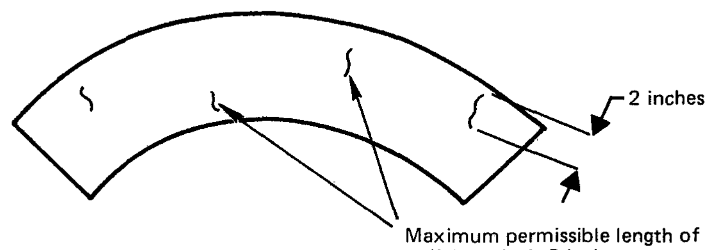

The formation of small clustered microcracks forming large low density regions shall be unacceptable.

2. Lithium hydride composition — The handling techniques used in the fabrication of the cast lithium hydride-container assemblies shall ensure that the purity of the lithium hydride conforms to section C-1-b of this specification.

3. Reinforcement — The lithium hydride shall be reinforced with a honeycomb structure. The honeycomb shall consist of 1-inch square cells with 1/2-inch diameter perforations on 3/4-inch centers in its walls. The honeycomb wall thickness shall be 0.001 inch. The honeycomb shall be oriented such that compliance with sections D-1-a and D-1-b of this specification is ensured.

4. Container distortion — The maximum allowable distortion shall be as shown on the applicable segment drawing in the as-fabricated and the as-cast condition:

Segment No. 7 Dwg. No. N00123007
Segment No. 2 Dwg. No. N00123008
Segment No. 3 Dwg. No. N00123009
Segment No. 1 Dwg. No. N00123010

5. Leaks — The maximum permissible leak rate of each shield sector is 10^{-4} standard cubic centimeters of helium per second with a pressure differential of 14.6 psi.

6. Thermocouples — The number of thermocouples that monitor the temperature of the lithium hydride during casting shall be limited to six (6) in the central 60 degrees in each shield section (see sketch). These thermocouples shall be located within four (4) inches of the bottom of the upper plate.

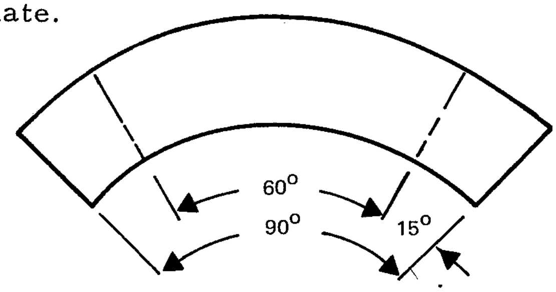

Additional thermocouples may be located in areas outside of the 60 degree central angle of the sector.

APPENDIX 3
CASTING FACILITY EQUIPMENT

The Atomic Energy Commission's Shield Casting Facility, located at the Atomics International Nuclear Field Laboratory, was used for casting the LiH shields. This facility contains the basic equipment needed for the casting process:

1) Powder-loading dry box — used for loading high-purity, granular LiH into the shield under a controlled protective atmosphere of nitrogen, containing a maximum of 3% oxygen, to eliminate the hazards of an explosive mixture of LiH dust and air, and to minimize the pickup of moisture.

2) Retort and retort base — to contain the shield during the casting cycle in an atmosphere of hydrogen, to prevent dissociation of the LiH at the high temperature

3) Large bell-type furnace — to heat the retort, shield, LiH, etc., to ~1400°F (1033°K)

4) Process and control components — to monitor and/or record temperatures, gas flow, gas pressure, and electrical power.

In addition, casting hardware, generally unique to each different size or geometry of LiH shield, is required, as follows:

a) Framework — consisting of vertical and horizontal members which support the shield and other components inside the retort during the casting process

b) Reservoir — an upper vessel, holding the pool of molten LiH which is supplied to the shield during the cooling process

c) Reservoir Loading Access — the stepped-down portion atop the reservoir, which mates with the dry box and provides a means of loading the LiH into the shield under the protective nitrogen atmosphere

d) Filler Tube — a bellows and tube assembly which provides a flexible connection between the reservoir and the shield

e) Thermocouples — stainless steel - sheathed, magnesia-insulated, Chromel-Alumel temperature sensors which monitor the temperatures inside the shield and reservoir during the cycle

f) Auxiliary (Trim) Heaters — stainless steel - sheathed, magnesia-insulated, Nichrome heaters which provide extra heat to selected regions, such as the filler tube and reservoir, during the casting cycle

g) Safety Container — a welded vessel which provides a means of containing the charge of molten LiH, in the event of a weld failure in the shield or the associated system.

APPENDIX 4
RADIOGRAPHIC PARALLAX TECHNIQUES

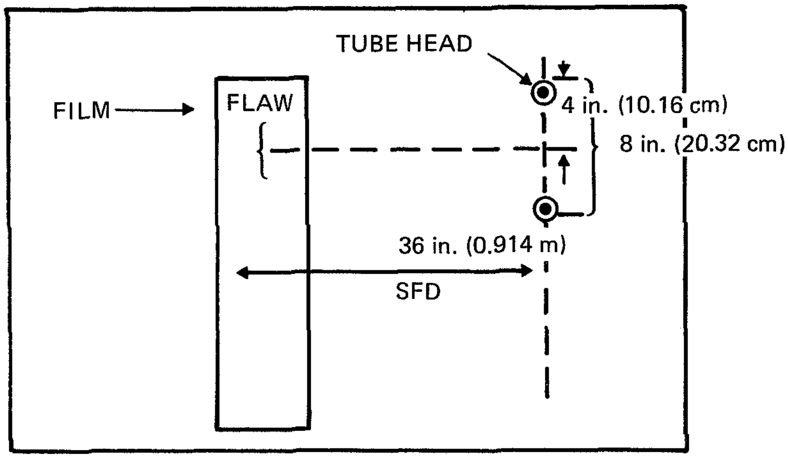

SEQUENCE:

1) Tube head centered on area of interest, shifted upward 4 in. (10.16 cm), and 75-sec exposure made
2) Tube head shifted 8 in. (20.32 cm) downward along perpendicular, and second exposure made on same film for same time
3) Flaw depth calculated, as shown in diagram.

$$L = D_1 - D_2 = T\left(\frac{B_1}{A + B_1} - \frac{B_2}{A + B_2}\right)$$

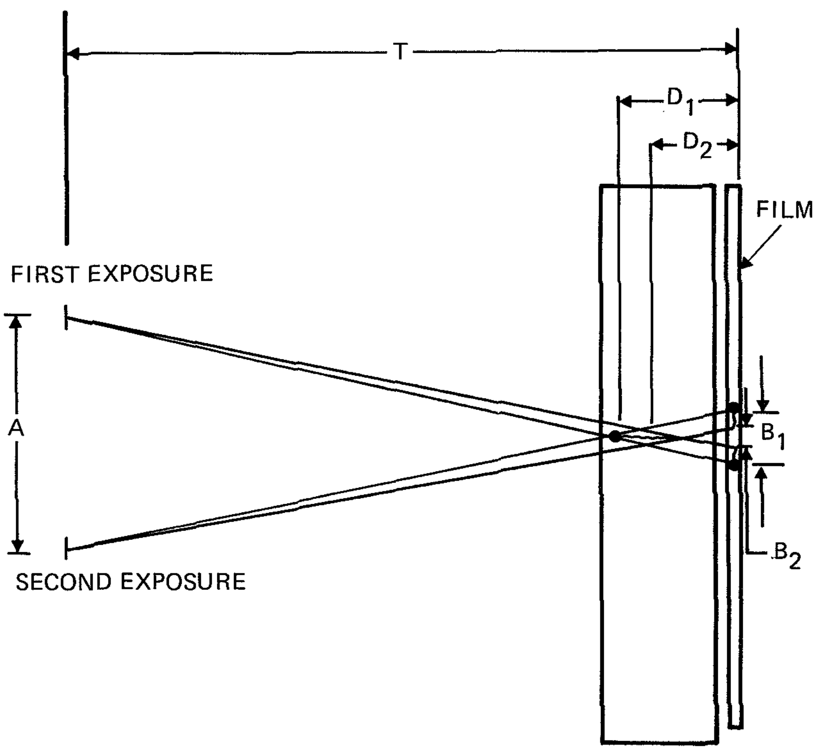

L = Crack length
D = Defect location from film plane
A = Tube head shift
B = Image shift on displacement
T = Distance, film to focal spot
B_1 = Maximum image shift
B_2 = Minimum image shift

6511-5611

APPENDIX 5
Segment No. 7

SURFACE CONTOUR NORMALITY

Contour Position	A		B		C		D		E		F		G		H	
Height from Bottom in. (cm)	Pre	Post	Pre	Post	Pre	Post	Pre	Post	Pre	Post	Pre	Post	Pre	Post	Pre	Post
	mil (mm)		mil (mm)		mil (mm)		mil (mm)		mil (mm)		mil (mm)		mil (mm)		mil (mm)	
0		0		0		0		0		0		0		0		0
0		0		0		0		0		0		0		0		0
4		50		10		8		80		50		80		80		0
10.16		1.27		0.254		0.203		2.03		1.27		2.03		2.03		0
8		10		20		-2		80		60		100		110		30
20.32		0.254		0.508		-0.051		2.03		1.52		2.54		2.79		0.762
12		30		30		-6		90		60		100		110		60
30.48		0.762		0.762		-0.152		2.29		1.52		2.54		2.79		1.52
16		50		70		-6		120		70		80		120		50
40.64		1.27		1.78		-0.152		3.05		1.78		2.03		3.05		1.27
20		62		100		-10		120		50		70		120		60
50.80		1.57		2.54		-0.254		3.05		1.27		1.78		3.05		1.52
24		62		90		-10		110		40		120		80		50
60.96		1.57		2.29		-0.254		2.79		1.02		3.05		2.03		1.27
28		59		90		-20		110		45		120		60		10
71.12		1.50		2.29		-0.508		2.79		1.14		3.05		1.52		0.254
32		50		85		-30		70		0		100		20		-20
81.28		1.27		2.16		-0.762		1.78		0		2.54		0.508		-0.508
36		43		80		-30		-10		-80		0		-80		-50
91.44		1.09		2.03		-0.762		-0.254		-2.03		0		-2.03		-1.27

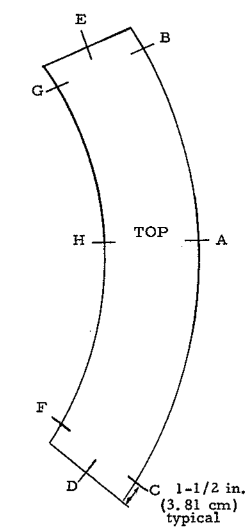

Negative (-) value means surface is convex or out, relative to the zero base position. Positive value means surface is concave or in, relative to the base.

SURFACE CONTOUR NORMALITY

Contour Position	A		B		C		D		E		F		G		H		I		J	
Height from Bottom in. (cm)	Pre	Post	Pre	Post	Pre	Post	Pre	Post	Pre	Post	Pre	Post	Pre	Post	Pre	Post	Pre	Post	Pre	Post
	mil (mm)		mil (mm)		mil (mm)		mil (mm)		mil (mm)		mil (mm)		mil (mm)		mil (mm)		mil (mm)		mil (mm)	
0	-	-	0	0	-	-	0	0	0	0	0	0	0	0	0	0	0	0	0	0
0	-	-	0	0	-	-	0	0	0	0	0	0	0	0	0	0	0	0	0	0
4	2	6	-4	-1	1	-10	10	29	10	41	-17	-6	-3	31	3	8	2	29	-25	-10
10.16	0.051	0.152	-0.102	-0.025	0.025	-0.254	0.254	0.737	0.254	1.04	-0.432	-0.152	-0.076	0.787	0.076	0.203	0.051	0.737	-0.635	-0.254
8	-3	-6	-12	19	14	-6	1	24	5	54	-22	-6	-1	59	13	28	-6	31	-33	-20
20.32	-0.076	-0.152	-0.305	0.483	0.356	-0.152	0.025	0.610	0.127	1.37	-0.559	-0.152	-0.025	1.50	0.330	0.711	-0.152	0.787	-0.838	-0.508
12	-10	-14	-21	24	12	-20	-3	32	0	70	-20	5	0	97	17	42	-13	36	-37	-26
30.48	-0.254	-0.356	-0.533	0.610	0.305	-0.508	-0.076	0.813	0	1.78	-0.508	0.127	0	2.46	0.432	1.07	-0.330	0.914	-0.940	-0.660
16	-14	-18	-30	19	24	-15	-13	34	-5	82	-23	7	3	115	0	38	-8	46	-35	-27
40.64	-0.356	-0.457	-0.762	0.229	0.610	-0.381	-0.330	0.864	-0.127	2.08	-0.584	0.178	0.076	2.92	0	0.965	-0.203	1.17	-0.889	-0.686
20	-11	-12	-26	-1	26	-17	-10	32	-7	80	-20	12	1	114	5	51	-21	28	-37	-36
50.80	-0.279	-0.305	-0.660	-0.025	0.660	-0.432	-0.254	0.813	-0.178	2.03	-0.508	0.305	0.025	2.90	0.127	1.30	-0.533	0.711	-0.940	-0.914
24	-5	2	-15	-7	19	-22	-8	27	-18	57	-18	16	-19	85	12	52	-23	24	-37	-42
60.96	-0.127	0.051	-0.381	-0.178	0.483	-0.559	-0.203	0.686	-0.457	1.45	-0.457	0.406	-0.483	2.16	0.305	1.32	-0.584	0.610	-0.940	-1.07
28	0	8	-10	-14	20	-12	-11	21	-21	40	-12	27	-31	47	8	44	-17	27	-35	-31
71.12	0	0.203	-0.254	-0.356	0.508	-0.305	-0.279	0.533	-0.533	1.02	-0.305	0.686	-0.787	1.19	0.203	1.12	-0.432	0.686	-0.889	-0.787
32	-2	-5	-9	-23	21	-4	-6	28	-14	32	-10	30	-41	15	8	43	-13	25	-29	-10
81.28	-0.051	-0.127	-0.229	-0.584	0.533	-0.102	-0.152	0.711	-0.356	0.813	-0.254	0.762	-1.04	0.381	0.203	1.09	-0.330	0.635	-0.737	-0.254
36	-13	-48	11	-45	2	-23	-31	-9	-32	-14	-18	-6	-22	3	-4	8	-9	5	-19	1
91.44	-0.330	-1.22	0.279	-1.14	0.051	-0.584	-0.787	-0.229	-0.813	-0.356	-0.457	-0.152	-0.559	0.076	-0.102	0.203	-0.229	0.127	-0.483	0.025

APPENDIX 6
SEGMENT NO. 1

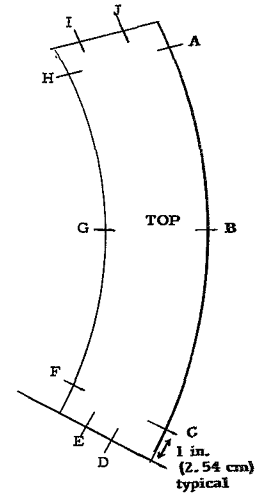

Negative (-) value means **surface is convex** or out, relative to the zero **base position.** Positive value means surface **is concave or** in, relative to the base.

APPENDIX 7
Segment No. 3

SURFACE CONTOUR NORMALITY

Contour Position	A		B		C		D		E		F		G		H		I		J	
Height from Bottom in. (cm)	Pre	Post	Pre	Post	Pre	Post	Pre	Post	Pre	Post	Pre	Post	Pre	Post	Pre	Post	Pre	Post	Pre	Post
	mil (mm)		mil (mm)		mil (mm)		mil (mm)		mil (mm)		mil (mm)		mil (mm)		mil (mm)		mil (mm)		mil (mm)	
0	-	-	0	0	-	0	0	0	0	0	0	0	0	0	0	0	0	0	0	0
0	-	-	0	0	-	0	0	0	0	0	0	0	0	0	0	0	0	0	0	0
4	5	23	-15	-35	-6	16	17	30	15	45	-16	2	9	27	0	19	-5	26	-5	14
10.16	0.127	0.584	-0.381	-0.889	-0.152	0.406	0.432	0.762	0.381	1.14	-0.406	0.051	0.229	0.686	0	0.483	-0.127	0.660	-0.127	0.356
8	3	24	-24	-58	-8	11	11	26	14	58	-10	8	20	56	2	27	-12	27	-21	-11
20.32	0.076	0.610	-0.610	-1.47	-0.203	0.279	0.279	0.660	0.356	1.47	-0.254	0.203	0.508	1.42	0.051	0.686	-0.305	0.686	-0.533	-0.279
12	4	19	-27	-70	-9	9	-5	9	9	65	0	23	26	79	-2	28	-12	37	-25	-21
30.48	0.102	0.482	-0.686	-1.78	-0.229	0.229	-0.127	0.229	0.229	1.65	0	0.584	0.660	2.01	-0.051	0.711	-0.305	0.940	-0.635	-0.533
16	1	10	-28	-66	-11	7	-9	3	3	68	11	35	25	81	-3	29	-10	45	-22	-11
40.64	0.025	0.254	-0.711	-1.68	-0.279	0.178	-0.229	0.076	0.076	1.73	0.279	0.889	0.635	2.06	-0.076	0.737	-0.254	1.14	-0.559	-0.279
20	-1	6	-30	-64	-6	17	-13	-3	-3	59	20	43	11	70	-12	20	-7	51	-16	-5
50.80	-0.025	0.152	-0.762	-1.63	-0.152	0.432	-0.330	-0.076	-0.076	1.50	0.508	1.09	0.279	1.78	-0.305	0.508	-0.178	1.30	-0.406	-0.127
24	-1	13	-32	-68	-8	15	-13	0	0	66	21	45	5	74	-11	22	-2	50	-14	-3
60.96	-0.025	0.330	-0.812	-1.73	-0.203	0.381	-0.330	0	0	1.68	0.533	1.14	0.127	1.88	-0.279	0.559	-0.051	1.27	-0.356	-0.076
28	-1	17	-27	-63	-10	15	-8	20	8	76	16	39	-10	53	-7	27	-4	38	-6	7
71.12	-0.025	0.432	-0.686	-1.60	-0.254	0.381	-0.203	0.508	0.203	1.93	0.406	0.991	-0.254	1.35	-0.178	0.686	-0.102	0.965	-0.152	0.178
32	-5	7	-25	-47	-18	-4	-10	31	1	73	14	35	-23	13	-12	25	2	36	6	25
81.28	-0.127	0.178	-0.635	-1.19	-0.457	-0.102	-0.254	0.787	0.025	1.85	0.356	0.889	-0.584	0.330	-0.305	0.635	0.051	0.914	0.152	0.635
36	-3	4	-8	-30	-25	-12	-28	5	-18	18	21	18	-2	-12	-27	-22	15	10	14	17
91.44	-0.076	0.102	-0.203	-0.762	-0.635	-0.305	-0.711	0.127	-0.457	0.457	0.533	0.457	-0.051	-0.305	-0.686	-0.559	0.381	0.254	0.356	0.432

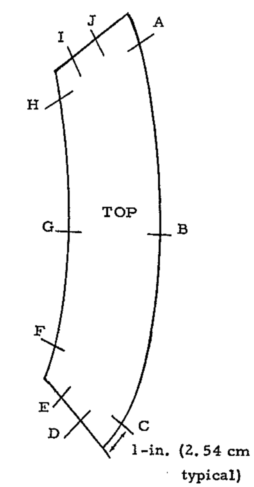

Negative (-) value means surface is convex or out, relative to the zero base position. Positive value means surface is concave or in, relative to the base.

APPENDIX 8
Segment No. 3

SURFACE CONTOUR NORMALITY

Contour Position	A		B		C		D		E		F		G		H		I		J	
Height from Bottom in. (cm)	Pre	Post	Pre	Post	Pre	Post	Pre	Post	Pre	Post	Pre	Post	Pre	Post	Pre	Post	Pre	Post	Pre	Post
	mil (mm)		mil (mm)		mil (mm)		mil (mm)		mil (mm)		mil (mm)		mil (mm)		mil (mm)		mil (mm)		mil (mm)	
0	-	-	0	0	0	-	0	0	0	-	0	0	0	0	0	0	0	0	0	0
0	-	-	0	0	-	-	0	0	0	0	0	0	0	0	0	0	0	0	0	0
4	2	5	-15	-13	5	-7	21	45	30	64	12	33	27	54	12	23	40	56	30	35
10.16	0.051	0.127	-0.381	-0.330	0.127	-0.178	0.533	1.14	0.762	1.63	0.305	0.838	0.686	1.37	0.305	0.584	1.02	1.42	0.762	0.889
8	4	17	-25	-23	5	-6	14	45	19	67	17	47	51	100	22	36	46	69	21	31
20.32	0.102	0.432	-0.635	-0.584	0.127	-0.152	0.356	1.14	0.482	1.70	0.432	1.19	1.30	2.54	0.559	0.914	1.17	1.75	0.533	0.787
12	2	18	-34	-35	1	-11	17	49	21	72	23	64	64	131	33	45	54	77	22	29
30.48	0.051	0.457	-0.864	-0.889	0.025	-0.279	0.432	1.24	0.533	1.83	0.584	1.63	1.63	3.33	0.838	1.14	1.37	1.96	0.559	0.737
16	-3	14	-43	-45	-6	-16	17	55	20	85	20	71	66	145	43	56	66	93	31	40
40.64	-0.076	0.356	-0.109	-1.14	-0.152	-0.406	0.432	1.40	0.508	2.16	0.508	1.80	1.68	3.68	1.09	1.42	1.68	2.36	0.787	1.02
20	-2	19	-45	-46	-8	-15	7	41	3	78	21	80	59	139	43	56	65	93	31	40
50.80	-0.051	0.483	-1.14	-1.17	-0.203	-0.381	0.178	1.04	0.076	1.98	0.533	2.03	1.50	3.53	1.09	1.42	1.65	2.36	0.787	1.02
24	-8	13	-44	-40	-8	-15	9	39	-4	64	8	73	39	113	33	53	71	103	46	51
60.96	-0.203	0.330	-1.12	-1.02	-0.203	-0.381	0.229	0.991	-0.102	1.63	0.203	1.85	0.991	2.87	0.838	1.35	1.80	2.62	1.17	1.30
28	-5	18	-43	-34	-13	-14	12	35	5	66	0	51	6	69	18	39	65	99	43	51
71.12	-0.127	0.457	-1.09	0.864	-0.330	-0.357	0.305	0.889	0.127	1.68	0	1.30	0.152	1.75	0.457	0.991	1.65	2.51	1.09	1.30
32	-3	19	-40	-26	-15	-15	9	34	-6	34	-14	27	-31	10	-4	13	58	84	41	52
81.28	-0.076	0.483	-1.02	-0.660	-0.381	-0.381	0.229	0.864	-0.152	0.864	-0.356	0.686	-0.787	0.254	-0.102	0.330	1.47	2.13	1.04	1.32
36	-1	-7	13	3	8	1	-22	-24	-36	-37	-28	-42	-38	-54	-33	-39	-26	-21	-16	-17
91.44	-0.025	-0.178	0.330	0.076	0.203	0.025	-0.559	-0.610	-0.914	-0.940	-0.711	-1.07	-0.965	-1.37	-0.838	-0.991	-0.660	-0.533	-0.406	-0.432

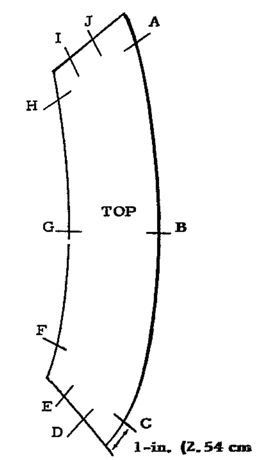

Negative (-) value means surface is convex or out, relative to the zero base position. Positive value means surface is concave or in, relative to the base.

DISTRIBUTION

Argonne National Laboratory
9700 South Cass Avenue
Argonne, IL 60440
Attn: E. N. Pettitt

Atomic Energy Commission
Washington, D.C. 20545
Attn: Hdqtrs. Library, Reports Section, MS G-017
Donald S. Beard
Ronald Anderson
C. McCallum

Atomic Energy of Canada Limited
Whiteshell Nuclear Research Establishment
Chemistry and Materials Science Division
Pinawa, Manitoba, Canada
Attn: R. F. Robertson, Division Director

Bettelle Memorial Institute
505 King Avenue
Columbus, OH 43201
Attn: W. Chubb
H. Russell

Donald W. Douglas, Inc.
2955 George Washington Way
Richland, WA 99352
Attn: Correspondence Control

General Electric Co.
Nuclear Systems Program
P.O. Box 15132
Cincinnati, OH 45215
Attn: H. C. Brassfield

General Electric Co.
Nuclear Thermionic Power Operation
P.O. Box 846
Pleasanton, CA 94566
Attn: J. Danko

General Electric Co.
Nuclear Energy Division (MC-328)
P.O. Box 1131
San Jose, CA 95108
Attn: Alleen Thompson

Gulf General Atomic, Inc.
P.O. Box 608
San Diego, CA 92112
Attn: L. Perry

Hittmann Associates, Inc.
Route 108
Columbia, MD 21043
Attn: H. Hagler

Jet Propulsion Laboratory
4800 Oak Grove Drive
Pasadena, CA 91103
Attn: J. F. Mondt

Los Alamos Scientific Laboratory
P.O. Box 1663
Los Alamos, NM 87544
Attn: Report Librarian, W. Reichelt

NASA Headquarters
Washington, D.C. 20546
Attn: RPE/J. Lazar
NS-1/J. Lynch
NS-1/P. Miller
NS-2/M. Klein, Manager SNSO
NS-1/C. Johnson

NASA Scientific and Technical Information Facility
Box 33
College Park, MD 20740
Attn: NASA Representative

NASA Manned Spacecraft Center
Houston, TX 77058
Attn: Librarian

Oak Ridge National Laboratory
Oak Ridge, TN 37830
Attn: A. Fraas
J. L. Scott
C. E. Clifford

Westinghouse Electric Corporation
Westinghouse Astronuclear Laboratory
P.O. Box 10864
Pittsburgh, PA 15236
Attn: J. G. Gallagher

Westinghouse Electric Corporation
Bettis Atomic Power Laboratory
West Mifflin, PA 15122
Attn: H. R. Warner

NASA Lewis Research Center
21000 Brookpark Road
Cleveland, OH 44135

Attn: Lewis Library (2)	MS 60-3
Report Control Office	MS 5-5
G. M. Ault	MS 3-13
D. J. Connolley	MS 49-2
R. E. English	MS 500-201
H. E. Hinckley	MS 500-309
L. V. Humble	MS 49-2
L. J. Kaszubinski (7)	MS 49-2
S. J. Kaufman	MS 49-2
M. H. Krasner	MS 49-2
N. T. Musial	MS 500-311
W. A. Paulson	MS 49-2
F. E. Rom	MS 106-1
H. O. Slone	MS 500-201